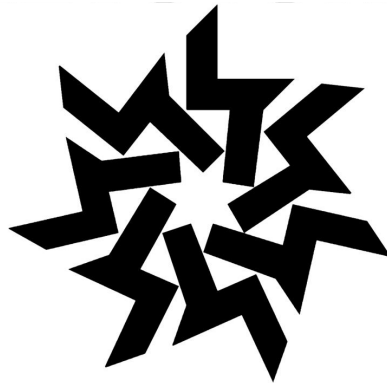


CEDAR 2017



Keystone Resort, Colorado

IT Studies Poster Session
Wednesday June 21, 2017

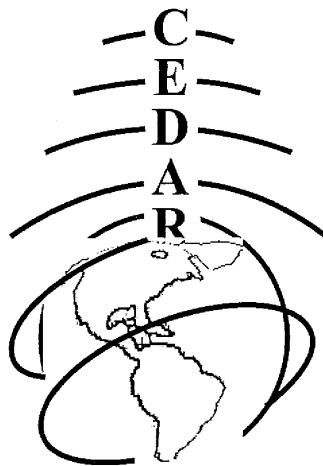


Table of Contents

DATA ASSIMILATION OR MANAGEMENT

DATA-01 - Understanding the variability in thermospheric nitric oxide flux using empirical orthogonal functions (EOFs) - by Sierra Flynn.....	1
DATA-02 - A Level 2 DMSP SSM Magnetometer & Auroral Boundary Dataset - by Liam Kilcommons	1
DATA-03 - Assessment of the impact of FORMOSAT-7/COMIC-2 GNSS RO observation on ionospheric specification and forecast using observing system simulation experiments - by Chih-Ting Hsu	2
DATA-04 - Real-Time Fitted Data for the Poker Flat Incoherent Scatter Radar - by Ashton Reimer	2
DATA-05 - Determining optimal setting for AMIENext procedure using cross validation - by Yining Shi	2

EQUATORIAL THERMOSPHERE OR IONOSPHERE

EQIT-01 - Impact of Midnight Thermosphere Dynamics on the Nighttime Mid- and Low-latitude Ionosphere - by Tzu-Wei Fang	3
EQIT-02 - Probing the Equatorial Plasmasphere with Jicamarca Long Pulse Experiments - by Sevag Derghazarian	3
EQIT-03 - Tropical ionization trough identified by Swarm satellite observations - by Woo Kyoung Lee	4
EQIT-04 - Equatorial thermospheric winds on quiet and storm times - by Luis Navarro.....	4
EQIT-05 - Simulation on the north-south ionospheric asymmetry during June solstice 2008 - by Chuan-Ping Lien	4
EQIT-06 - Estimates of the equatorial evening plasma vortex using climatological models - by Sam Shidler	5
EQIT-07 - Calculating the 3-dimensional current in the ionosphere and its associated magnetic perturbation - by Astrid Maute	5
EQIT-08 - Characteristics of Equatorial Electrojet Variability and its Consequences in Low-Latitude Ionosphere - by Sovit Khadka.....	6
EQIT-09 - Interactive Ion-Neutral Dynamics in the Low Latitude Evening Ionosphere - by William Evonosky	6
EQIT-10 - Pre-sunrise uplift in vertical plasma drift using TIEGCM-ICON simulation - by Tiju Mathew	7
EQIT-11 - Studying the variability of 150 km Echoes - by Abhishek Desai	7
EQIT-12 - Multi-static HF radar system in Peru - by Alexander Valdez Portocarrero	8

IRREGULARITIES OF IONOSPHERE OR ATMOSPHERE

IRRI-01 - Characterization of Shortwave Fadeout seen in Daytime SuperDARN Ground-Scatter Observations - by Shibaji Chakraborty.....	8
IRRI-02 - Variations in equatorial spread F between conjugate sites - by Dustin Hickey	9
IRRI-03 - On the Relationship between Sporadic-E and ENSO Observed by FORMOSAT-3/COSMIC - by Pei-yun Chiu	9
IRRI-04 - First experiments at the (new) UAF-HAARP facility: preliminary artificial airglow results and guidelines for future experiments - by Christopher Fallen	9
IRRI-05 - In-situ and ground-based observations of equatorial plasma irregularities and implications for Spread F dynamics - by Dev Joshi	10
IRRI-06 - A Global Study of Ionospheric Irregularities during Daytime at the Magnetic Dip Equator using SCINDA Ground-based and Radio Occultation Measurements - by Aramesh Seif.....	10
IRRI-07 - Reconstruction of the GPS phase scintillation during a magnetospheric substorm - by Sebastijan Mrak	11

IRRI-08 - Detection of Spread-F, foF2 values and Planetary and Gravity Wave Signatures using Digisonde and VIPIR instruments and their comparison with COSMIC-I/FORMOSAT-3 data - by Preeti Bhaneja	12
IRRI-09 - Equatorial Plasma Bubbles: variations of occurrence and spatial scale in local time, longitude, season and solar activity - by Jonathon Smith	12
IRRI-10 - Deployable Satellite Receiver Node Design to Measure Ionospheric Scintillation - by Xiaoyu Han	12
IRRI-11 - Sensing Ionospheric Irregularities with a GNSS Receiver Array during a Geomagnetic Storm - by Yang Su	13
IRRI-12 - Radar Imaging with MaxEnt for Manastash Ridge Radar - by Marcos Inonan	13
IRRI-13 - June solstice equatorial spread F: On the role of weak vertical plasma drifts - by Weijia Zhan	14
IRRI-14 - Zonal Structure in All Sky Images of Auroral Features - by Robert Finan	14

LONG TERM VARIATIONS OF THE IONOSPHERE-THERMOSPHERE

LTVI-01 - Observed increase in geocoronal hydrogen emissions - by Susan Nossal	14
LTVI-02 - Diurnal variation of atomic hydrogen density in the terrestrial upper atmosphere - by Yamuna Phal	15
LTVI-03 - Spectral Analysis of the Neutral Wind Components over Arecibo based on Five Consecutive Years (2012-2017) of Fabry-Perot Observations - by Eframir Franco-Diaz	15
LTVI-04 - The long-term trends in thermospheric mass density and ionospheric total electron content - by Rong Tsai-Lin	16

MIDLATITUDE THERMOSPHERE OR IONOSPHERE

MDIT-01 - Wind Field Plotting for Red and Green Line Scanning Doppler Imager Data - by Kylee Branning	16
MDIT-02 - Arecibo Observatory - HF facility and diagnostics - by Eliana Nossa	16
MDIT-03 - Ionosonde-Based Indices for Improved Representation of Solar Cycle Variation in the International Reference Ionosphere Model - by Steven Brown	17
MDIT-04 - The Arecibo Observatory Remote Optical Facility (AO-ROF) in Culebra Island, Puerto Rico: Current Status and Future Projects - by Pedrina Santos	17
MDIT-05 - O-O+ momentum imbalance in the topside ionosphere: implications for bias in MSIS oxygen density specification - by Pratik Joshi	17
MDIT-06 - Statistical Study of Nightside Quiet Time Subauroral Ionospheric Convection Observed by the North American Midlatitude SuperDARN Radars - by Maimaitirebike Maimaiti	18
MDIT-07 - Longitudinal structure in electron density at mid-latitudes: upward-propagating tidal effects - by kedeng Zhang	18
MDIT-08 - Helium Structure in the Upper Thermosphere - by Torfinn Johnsrud	19
MDIT-09 - Seeking Lagrangian Coherent Structures in Ionospheric Plasma Drift Flows - by Ningchao Wang	19

MAGNETOSPHERE-IONOSPHERE-THERMOSPHERE COUPLING

MITC-01 - Model-data comparison of neutral wind impacts on high-latitude ionospheric upflows - by Meghan Burleigh	20
MITC-02 - Magnetosphere-ionosphere-thermosphere coupling through H redistribution driven by geomagnetic storms - by Jianqi Qin	20
MITC-03 - On the relation between soft electron precipitations in the cusp 1 region and solar wind coupling functions - by Tong Dang	21
MITC-04 - Effects of SAPS on thermospheric wind and density during the 17 March 2013 storm - by Cheng Sheng	21
MITC-05 - SAPS simulation with GITM_RCM coupled Model - by Yang Lu	22
MITC-06 - Observations of the midlatitude trough and its relationship to subauroral ion drifts (SAID) - by Russell Landry	22
MITC-07 - Statistical Comparison of the Magnetopause Distance and CPCP for Global MHD Models - by Agnit Mukhopadhyay	22

MITC-08 - Low-altitude ion heating with downflowing and upflowing ions - by Yangyang Shen	23
MITC-09 - Swarm Observation of Field-Aligned Currents in Multiple Arc System - by Jiashu Wu.....	23
MITC-10 - Impact of the electric field variability on the upper atmosphere during the geomagnetic storm - by Qingyu Zhu.....	24

PLANETARY STUDIES

PLAN-01 - Comparative Aeronomy: Molecular Ionospheres at Earth and Mars - by Michael Mendillo	24
PLAN-02 - Using the Development Process of the Venus Global Ionosphere-Thermosphere Model to Understand the Importance of Planetary Attributes on Earth’s Atmosphere - by Emily Judd.....	25

POLAR AERONOMY

POLA-01 - Kinetic modeling of auroral ion Outflows observed by the VISIONS sounding rocket - by Robert Albarran	25
POLA-02 - Imaging Fabry-Perot Observations of Thermospheric Dynamics in Antarctica - by Mark Conde	26
POLA-03 - Statistical Characteristics of Ionospheric Polar Cap Patches Observed by RISR-C - by Jiaen Ren.....	26
POLA-04 - Seasonal dependence of geomagnetic active time northern high-latitude upper thermospheric winds - by Manbharat Dhadly.....	26
POLA-05 - Characterizing the Polar Topside Ionosphere - by Aaron Bunch	27
POLA-06 - Occurrence of ion upflow associated with ion/electron heating in the polar cap and cusp regions - by Eun-Young Ji	27
POLA-07 - Exploring the high-latitude thermosphere responses to IMF By reversal - by Dongjie Guo	27
POLA-08 - Measuring F-region ion-neutral coupling in response to increases in auroral precipitation - by Andrew Kiene	28
POLA-09 - Thermospheric wind variations at substorm onset: Multi-event study using a Fabry-Perot interferometer at Tromsø, Norway - by Heqiucen Xu	28
POLA-10 - High Resolution Case Studies of Giant Auroral Undulations - by Michael Ahrns	29
POLA-11 - Preliminary Data Analysis of ISINGLASS Campaign Launches - by Robert Clayton.....	29

SOLAR TERRESTRIAL INTERACTIONS IN THE UPPER ATMOSPHERE

SOLA-01 - Tomographic estimation of exospheric hydrogen density distributions - by Gonzalo Cucho-Padin	30
SOLA-02 - Studying the response of the low-ionosphere to solar Long Duration Gamma-Ray Flares (LDGRF) - by Alessandra Abe Pacini	30
SOLA-03 - Effects of Space Weather on the Estimation of Thermospheric Density - by Timothy Kodikara.....	30
SOLA-04 - Initial Validation of CTIPe Neutral Winds using GOCE Satellite Observations - by Mariangel Fedrizzi	31
SOLA-05 - Ionosphere-thermosphere modeling in a forecastable mode: case study of the June 2012 geomagnetic storm - by Xing Meng	31
SOLA-06 - Statistical study of the traveling ionospheric disturbances generated by solar terminator based on Dynasonde data - by Huan Song.....	32
SOLA-07 - Analysis of the August 2017 Eclipse’s Effect on Radio Wave Propagation Employing a Raytrace Algorithm - by Magdalena Moses.....	32

CEDAR Workshop - IT Studies Session Abstracts
Day 2 – Wednesday, June 21, 2017

DATA ASSIMILATION OR MANAGEMENT

DATA-01 - Understanding the variability in thermospheric nitric oxide flux using empirical orthogonal functions (EOFs) - by Sierra Flynn

Status of First Author: Student IN poster competition, MS

Authors: S. Flynn, T. Matsuo, D. Knipp, M. Mlynczak, and L. Hunt

Abstract: Quantifying the spatial and temporal variability of nitric oxide emissions in the thermosphere using eigenmodes will increase the understanding of how upper atmospheric nitric oxide behaves, and could be used to increase the accuracy of future space weather and climate models. Nitric oxide flux from 100-250 km altitude taken from 13 years of data observed by the SABER instrument onboard the TIMED satellite is decomposed into five EOFs and their amplitudes to: 1) determine the strongest modes of variability in the data set, and 2) develop a compact model of nitric oxide flux. The first five EOFs account for 85% of the variability in the data, and their uncertainty is verified using cross-validation analysis. Although these linearly independent EOFs are not necessarily independent in a geophysical sense, the first three EOFs correlate strongly with different geophysical processes. The first EOF correlates strongly with Kp and F10.7, suggesting that geomagnetic storms and solar weather account for a large portion of nitric oxide flux variability. EOF 2 shows annual variations, and EOF 3 correlates with solar wind parameters. Using these relations, an empirical model of the EOF amplitudes can be derived, which could be used as a predictive tool for future nitric oxide emissions. We illustrate the nitric oxide model and discuss the geophysical associations of the EOFs.

DATA-02 - A Level 2 DMSP SSM Magnetometer & Auroral Boundary Dataset - by Liam Kilcommons

Status of First Author: Non-student

Authors: Liam Kilcommons, Robert Redmon, and Delores Knipp

Abstract: We have developed a method for reprocessing the multi-decadal, multi-spacecraft Defense Meteorological Satellite Program Magnetometer (DMSP SSM) dataset and have applied it to fifteen spacecraft-years of data (DMSP Flight 16-18, 2010-2014). This Level-2 dataset improves on other available SSM datasets with recalculated spacecraft locations and magnetic perturbations, artifact signal removal, and representations of the observations in geomagnetic coordinates.

We validate our Level-2 SSM data by showing favorable comparisons between mid-latitude nightside Level-2 SSM data with DMSP MAG 1 (Alken et al. [2014]). DMSP MAG 1 is a DMSP SSM-derived scientific-grade main field model which employed an alternative post-processing scheme. We also show comparisons between our Level-2 SSM data and other publicly available DMSP SSM data sets.

Using coincident data from the DMSP precipitating electrons and ions instrument (SSJ4/5), we detect the in-situ auroral boundaries with an improvement to the Redmon et al. [2010] algorithm. We embed the resulting location of the aurora and an accompanying figure of merit in the Level-2 SSM data product, thus meeting a long-standing community need of providing context, (poleward, inside or equatorward of the auroral oval) for magnetic perturbations and potentially other measurements made by DMSP.

We also show several uses and research directions enabled by the new dataset including expressions of DMSP observations in dynamic auroral boundary coordinates, and estimates of field aligned currents and Joule heating.

DATA-03 - Assessment of the impact of FORMOSAT-7/COMIC-2 GNSS RO observation on ionospheric specification and forecast using observing system simulation experiments - by Chih-Ting Hsu

Status of First Author: Student IN poster competition, PhD

Authors: Chih-Ting Hsu, Tomoko Matsuo, Xinan Yue, and Jann-Yenq Liu

Abstract: The Formosa Satellite-7/Constellation Observing System for Meteorology, Ionosphere and Climate-2 (FORMOSAT-7/COSMIC-2) GNSS RO payload can provide global observations of slant total electron content (sTEC) with unprecedentedly high spatial temporal resolution. By using observing system simulation experiments, we can quantitatively assess the impact of FORMOSAT-7/COSMIC-2 GNSS RO data on ionospheric specification and forecast. For this purpose, a coupled model of the Global Ionosphere Plasmasphere and the Thermosphere Ionosphere Electrodynamics General Circulation Model is incorporated into the NOAA ensemble Kalman filter data assimilation system. In ensemble Kalman filtering, it is critical to minimize the effects of sampling errors on the ensemble-based estimation of the correlation between observations and model states, in order to obtain high quality assimilation analysis. This presentation will demonstrate how an auxiliary ensemble Kalman filtering technique designed specifically for the FORMOSAT-7/COSMIC-2 sTEC observations can enhance the impacts of FORMOSAT-7/COSMIC-2 GNSS RO data on ionospheric specification and forecast.

DATA-04 - Real-Time Fitted Data for the Poker Flat Incoherent Scatter Radar - by Ashton Reimer

Status of First Author: Non-student

Authors: Ashton S. Reimer, Roger H. Varney, and Todd A. Valentic

Abstract: The Poker Flat Incoherent Scatter Radar (PFISR) is an Advanced Modular Incoherent Scatter Radar (AMISR) located on the Poker Flat Research Range (PFRR) in Alaska. PFISR typically operates in multiple beam modes, taking advantage of the electronic beam steering capabilities of the AMISR architecture. The multiple beam capability produces a large amount of data that provides a significant computational challenge for real time processing. Historically, the unavailability of cheap computational resources have prevented real time fitting of PFISR data, but these challenges are no longer present with modern multi-core processors and parallel processing.

Real time fitted data products from an Incoherent Scatter Radar (ISR) are excellent tools for ionospheric scientific campaigns. Real time ISR data can provide context that may be critical to campaign decision making, such as deciding whether or not ionospheric conditions are optimal for launching a sounding rocket.

Here we present a system architecture for processing PFISR data in real time. The real time products include low-level data (signal-to-noise ratio, uncorrected electron density, and a rough estimate of the line-of-sight velocity), fitted data products in each beam produced by fitting the autocorrelation functions (corrected electron density, electron temperature, ion temperature, and line-of-sight velocity), and derived products produced by combining data from multiple beams (vector velocities and E-region neutral winds). The PFISR real-time system was initially deployed in February 2017, and real time fitted PFISR data supported the February 13, 2017 to March 3, 2017 PFRR sounding rocket campaign.

DATA-05 - Determining optimal setting for AMIENext procedure using cross validation - by Yining Shi

Status of First Author: Student IN poster competition, PhD

Authors: Yining Shi, Delores Knipp, Tomoko Matsuo, Liam Kilcommons, and Brian Anderson

Abstract: The Assimilative Mapping of Ionospheric Electrodynamics Next (AMIENext) procedure developed by Matsuo et al. (2015) generates magnetic potential and field-aligned current (FAC) patterns in the high-latitude region by assimilating magnetic perturbation data from Active Magnetosphere and Planetary Electrodynamics Response Experiment (AMPERE) using optimal interpolation (OI) method. OI method updates the prior knowledge of states with observations using Bayesian inference. Therefore, assimilation results vary considerably with the choice of settings that include background model, prior covariance, observation error and parameters used in the procedure. We evaluate the performance of AMIENext under different settings using cross validation against AMPERE and DMSP magnetic perturbation data. An optimal setting for the procedure is determined based on the validation results. We study the procedure's settings and their performance for various solar wind and magnetosphere-ionosphere coupling conditions to determine corresponding changes needed to produce the optimal result. Primary results show that using AMPERE data mean as the background instead of the empirical model developed by Weimer (2005) gives better agreement between the estimations and observations. How well the data matches the background may depend on conditions and needs further investigation.

EQUATORIAL THERMOSPHERE OR IONOSPHERE

EQIT-01 - Impact of Midnight Thermosphere Dynamics on the Nighttime Mid- and Low-latitude Ionosphere - by Tzu-Wei Fang

Status of First Author: Non-student

Authors: T.-W. Fang, R. Akmaev, Y.-C. Lin, T. Fuller-Rowell, and A. D. Richmond

Abstract: Simulations using the coupled Whole Atmosphere Model and Global Ionosphere Plasmasphere Model (WAM/GIP) have successfully reproduced the unusual upward drift during the post-midnight period (~2-3 LT) that were observed by C/NOFS satellite during the recent solar minimum. Model produces significant day-to-day variability in the nighttime equatorial ionosphere and also reveals strong seasonal and longitudinal dependence of the nighttime upward drift. Our analysis indicates that the upward drifts are driven by thermosphere dynamics associated with the midnight temperature maximum (MTM). The MTM locally reverses the typical large-scale zonal and meridional wind pattern, in turn affecting the nighttime F-layer electrodynamics. The longitudinal variation of the drifts depends on the magnitude and position of the MTM peak relative to the magnetic equator. In this poster, we will present the morphology and characteristics of the post-midnight upward drift shown in the simulations and explain its causal mechanism. Additionally, simulation of growth rate of Rayleigh–Taylor instability associated with the nighttime upward drift and brightness waves produced by the MTM will also be shown.

EQIT-02 - Probing the Equatorial Plasmasphere with Jicamarca Long Pulse Experiments - by Sevag Derghazarian

Status of First Author: Student IN poster competition, PhD

Authors: Sevag Derghazarian, Dr. David Lee Hysell

Abstract: The Jicamarca observatory was built more than 50 years ago in order to test the growing field of incoherent scatter from upper atmospheric plasma. In the early days of the facility, high altitude experiments were routinely performed leading to electron density measurements from the inner magnetosphere (plasmasphere), but were soon discontinued. Recently, with the advent of the long pulse technique, high altitude experiments were revived, exploring and analyzing this lesser known region of the upper atmosphere.

In this poster, we explain the process of deriving plasmasphere parameters using the long pulse technique applied to high altitude experiments (approximately $L=2$). The parameters are calculated using experimental data incorporated into a full profile analysis that yields estimates of electron density, electron and ion temperature and light ion composition at varying altitudes. Inverse methods are employed for transforming measured lag products into autocorrelation functions and subsequently meaningful parameters. Additionally, the process involves noise removal algorithms based on order statistics to account for the scattering caused by moving space debris and satellites.

EQIT-03 - Tropical ionization trough identified by Swarm satellite observations - by Woo Kyoung Lee

Status of First Author: Non-student

Authors: Woo Kyoung Lee, Hyosub Kil

Abstract: The plasma density minima in the equatorial region (equatorial ionization trough) and subauroral region (mid-latitude ionization trough) are well known phenomena. However, little is known about the plasma density minimum in the tropical region. We call this new feature “tropical ionization trough”. From the measurements of the electron density by Swarm satellites, we have identified the occurrence of the tropical ionization trough near ± 20 degree magnetic latitudes. It preferentially occurs after midnight in both hemispheres. Our study attempts to quantify the local time, season, and longitudinal variation of the occurrence and intensity of the trough by analyzing the Swarm satellite observations in 2014-2016. We also investigate the occurrence altitude of the trough by analyzing the vertical electron density profiles retrieved from the observations of the Constellation Observing System for Meteorology, Ionosphere, and Climate/GPS radio occultation data. The combined effects of neutral winds and geomagnetic field configuration is investigated by conducting Sami2 is Another Model of the Ionosphere model simulations.

EQIT-04 - Equatorial thermospheric winds on quiet and storm times - by Luis Navarro

Status of First Author: Student IN poster competition, PhD

Authors: Luis Navarro, Bela Fejer

Abstract: Solar wind effects under the magnetosphere-ionosphere system can generate disturbances on radio and satellite communications. Therefore, the study on how these systems are coupled is critical to understand, and eventually forecast, its dynamics and consequences

Different instrumentation has been deployed to reach the goal just stated. Among them, a network of Fabry Perot Interferometer was setup in the Central Region of Peru and reach up to 47535 hours of operations. This instrumentation is capable of measuring the state of the neutral thermosphere by use of the Doppler shift and Doppler broadening of the red oxygen line in the airglow from which we are able to obtain Zonal/Meridional wind speed and Temperature. This data was classified into quiet and storm time based on the geophysical Kp index and contrasted with different empirical models like HWM14 and DWM07 for quiet and storm times. An analysis of the neutral atmosphere dynamics for both times is presented.

EQIT-05 - Simulation on the north-south ionospheric asymmetry during June solstice 2008 - by Chuan-Ping Lien

Status of First Author: Non-student

Authors: Chuan-Ping Lien¹, Charles Lin¹, Chia-Hung Chen¹, Chi-Yen Lin³, and J. D. Huba⁴

¹ Department of Earth Science, National Cheng-Kung University, Tainan, Taiwan

² Graduate Institute of Space Science, National Central University, Taoyuan, Taiwan

³ Graduate Institute of Space Science, National Central University, Taoyuan, Taiwan

4 Plasma Physics Division, Naval Research Laboratory, Washington, District of Columbia, USA

Abstract: In this study, three-dimensional ionosphere electrodynamic model, NRL-SAMI3, is utilized to simulate the north-south ionospheric asymmetry during June solstice 2008. To further investigate tidal wind effects to the asymmetry of EIA, the neutral wind are specified by the different version of empirical Horizontal Wind Model (HWM14 and HWM93). The simulation results show that the clear asymmetry in EIA and that the transition times are around 1300-1400LT and 1500-1600LT on 120oE sector, with the neutral wind given by HWM14 and HWM93 respectively. The tidal-decomposition analysis further suggests that the transition time of EIA asymmetry depends on the phase of migrating semi-diurnal tidal component (SW2) of the meridional neutral wind.

EQIT-06 - Estimates of the equatorial evening plasma vortex using climatological models - by Sam Shidler

Status of First Author: Student IN poster competition, PhD

Authors: Sam Shidler, Fabiano Rodrigues

Abstract: The evening plasma vortex is an important electrodynamic feature of the low-latitude F-region ionosphere. It is the result of a complex thermosphere-ionosphere interaction, and controls the horizontal and vertical transport of ionospheric plasma. More recently, it has been associated with the development of interchange plasma instabilities and equatorial spread F.

Here, we present results of an investigation of the ability of combining readily available thermospheric and ionospheric climatological models (IRI, Scherliess and Fejer (1992) vertical plasma drift model, MSIS, HWM and IGRF) to produce the evening plasma vortex. For that purpose, we followed the two-dimensional formulation of the ionospheric electrodynamics described by Haerendel et al. (1992). They showed that the three-dimensional equations governing ionospheric currents can be simplified to a two dimensional problem. This simplification assumes that the electric potential along magnetic field lines is constant and that electric fields in the equatorial plane map along these field lines. This is a reasonable assumption for the E- and F- regions of the low-latitude ionosphere where the parallel conductivity is several orders of magnitude larger than the perpendicular Pedersen and Hall conductivities. A further simplification is made in our present analysis by neglecting the effects of the vertical integrated current. Using TIE-GCM results, Rodrigues et al. (2012) showed that evening plasma vortex can still be reproduced even when the vertical current is neglected.

During this poster presentation, we will describe our numerical calculation, provide results of the simulation outputs and discuss our results of the two-dimensional plasma flow patterns in the magnetic equatorial plane.

EQIT-07 - Calculating the 3-dimensional current in the ionosphere and its associated magnetic perturbation - by Astrid Maute

Status of First Author: Non-student

Authors: Astrid Maute, Art Richmond

Abstract: In the last several decades Low Earth Orbit (LEO) satellites have provided extensive magnetic measurements to advance our understanding of the complex ionospheric current system. Interpreting the measured magnetic field and its associated current is still challenging since the measured magnetic field reflects the influence of various current sources. At high latitude ionospheric currents are mainly driven by the magnetosphere-ionosphere coupling through ion convection and field-aligned current. At mid- and low latitude the collisional interaction between thermospheric winds and ions is important and sets up electric fields and currents. Smaller low latitude current is produced by gravity and plasma pressure gradient forces. The later two currents originate at LEO height, and therefore the height variation of the current has

to be considered to accurately determine the LEO magnetic perturbation. Knowledge about the characteristics of these currents and their associated magnetic perturbation is important for studies analyzing day and evening low latitude LEO magnetic perturbations.

In this presentation we will introduce a numerical model capable of calculating the 3D, divergence-free, ionospheric current system and its associated magnetic perturbation at LEO altitude. We apply this model to examine the current system and the magnetic perturbations, and especially focus on the effects of gravity and plasma pressure gradient forces with respect to local time, season and solar cycle. With the new model we can evaluate the diamagnetic approximation by comparing with the magnetic perturbation derived from considering the simulated 3D current system. We will discuss the value of the simulation results with respect to studies based on LEO magnetic field measurements.

EQIT-08 - Characteristics of Equatorial Electrojet Variability and its Consequences in Low-Latitude Ionosphere - by Sovit Khadka

Status of First Author: Student NOT in poster competition, PhD

Authors: Cesar E. Valladares, Endawoke Yizegaw

Abstract: The equatorial electrojet (EEJ) is a narrow latitudinal ($\pm 3^\circ$) band of intense current flowing at the ionospheric E region, and produces strong geomagnetic field variations during the daytime over the dip equator. The unique physical properties of the equatorial ionosphere (e.g. EEJ) hold great promise for unraveling the governing mechanism of the dayside ionospheric dynamics and the onset of the enigmatic plasma structures in the geospace environment. This report provides an overview of the characteristics of the narrow longitudinal and seasonal variability of the EEJ, including its temporal variation, using magnetometer observations. A case and statistical study of the EEJ strengths is presented using four pairs of magnetometers, one located at the dip equator and another off the dip equator ($\pm 6^\circ$ to $\pm 9^\circ$ away) in the American low-latitude regions. Our results reveal that the EEJ strength looks weaker at the eastern longitudes than in the western sector in the American low latitudes. The variation of the morning depression and the effect of its unique shape, as well as variation of the equatorial geomagnetic field curve on the EEJ, will also be discussed. The consequences of the variability of the low-latitude ionospheric current observed in the scenario of vertical drifts, the equatorial anomaly, as well as GPS-TEC distributions, will be investigated. The role of the EEJ as a proxy parameter for forecasting the ionospheric dynamics with precise estimates of the time and location will also be examined.

EQIT-09 - Interactive Ion-Neutral Dynamics in the Low Latitude Evening Ionosphere - by William Evonosky

Status of First Author: Student IN poster competition, PhD

Authors: William Evonosky, Dr. Art Richmond, Dr. Tzu-Wei Fang, and Dr. Astrid Maute

Abstract: We examine the forces that determine zonal wind structure in the low-latitude evening thermosphere and its relation with ion-neutral coupling. Forces are calculated using the Thermosphere-Ionosphere-Electrodynamics General-Circulation Model coupled with the Global Ionosphere-Plasmasphere model. At 19 LT, the horizontal pressure gradient dominates the net acceleration of neutral winds below ~ 220 km while it tends to be offset by ion drag and viscosity higher up. The eastward pressure-gradient acceleration above 200 km increases approximately linearly with height, and tends to be similar for different latitudes and different levels of solar activity. We surmise that the latitude uniformity of the eastward pressure gradient is maintained by the tendency for divergent/convergent north-south winds to rapidly equalize pressure differences. The pressure-gradient and ion-drag forces in the central F region approximately balance for field lines that pass through the equatorial ionization anomaly, but viscosity is an important additional force elsewhere. For different night-time ionization levels, ion-drag acceleration tends to remain constant while ion and neutral velocities change to conserve the difference between them. The presence of a low-latitude evening-time vertical shear in the zonal wind is associated primarily with a

strong eastward pressure-gradient acceleration at high altitude that reverses the day-time westward wind, and a weak low-altitude pressure-gradient acceleration of either eastward or westward direction that fails to reverse the low-altitude westward wind present in the afternoon.

EQIT-10 - Pre-sunrise uplift in vertical plasma drift using TIEGCM-ICON simulation - by Tiju Mathew

Status of First Author: Student NOT in poster competition, PhD

Authors: T. J. Mathew^{1,3}, T.-W Fang², Astrid Maute³ and A. D. Richmond³

1. Department of Physics, Christian College, Chengannur, Kerala, India
2. Cooperative Institute for Research in Environmental Sciences, University of Colorado, USA
3. High Altitude Observatory, National Center for Atmospheric Research, Boulder, USA.

Abstract: The observations from low-latitude stations, Trivandrum (using multi-frequency HF Doppler radar) and Jicamarca (using Incoherent scatter radar) show that, the vertical plasma drift observed during early morning hours is characterised by an upward drift prior to sunrise followed by a downward drift. In the present work, days on which pre-sunrise uplift was present in the vertical drift, observed at Jicamarca Radio Observatory in 2009 are identified and Thermosphere Ionosphere Electrodynamic General Circulation Model (TIEGCM) of NCAR is used to interpret the causal mechanism of the pre-sunrise uplift. For the TIEGCM simulations, instead of using the Global Scale Wave Mode (GSWM), the 27-day averaged diurnal perturbations based on Thermosphere Ionosphere Mesosphere Electrodynamic General Circulation Model (TIMEGCM) and climatological background is imposed at the lower boundary (Maute, Space Sci. Rev., 2017).

Running the TIEGCM under different settings, (1) Winds at all altitudes are switched on ((E+F)_Dynamo), (2) Winds below 150 km is switched off (F_Dynamo) and (3) Winds above 150 km is switched off (F_Ddynamo), results clearly show that, the contributions of F-region dynamo in producing the pre-sunrise uplift and E-region dynamo in the subsequent downward drift are significant. Simulations also demonstrate the strong impact of high latitude potential on producing the uplift during night time. In this poster, the comparisons between observations and simulations will be shown and the mechanisms that lead to the pre-sunrise upward drift will be discussed in detail.

EQIT-11 - Studying the variability of 150 km Echoes - by Abhishek Desai

Status of First Author: Student IN poster competition, PhD

Authors: Abhishek Desai (Clemson), Gerald Lehmacher (Clemson), Eran Kudeki (Illinois), and Pablo Reyes (Illinois)

Abstract: Daytime VHF echoes from the F1 region (from ~130 to 200 km) are an everyday, normal occurrence in the tropical ionosphere. The 150-km echoes exhibit a very regular “necklace” pattern with descent in the morning and ascent in the afternoon suggesting a close relationship with electron density. Many vertically stacked layers are present separated by narrow, “forbidden” regions of no backscatter. We have found that the characteristic arrangement of these layers is the same every day, but shifts vertically depending on the season.

We will present the results of our data analysis of the asymmetrical “necklace” shape, the depth of the layers, and day-to-day and seasonal variations using high-resolution observations made by the Jicamarca radar in 2014 to 2016. We have traced at least three “forbidden” regions with no backscatter, which give us characteristic height-vs-time curves for each day. The time and altitude of the lowest point for each curve may help us understand the generation mechanisms of these echoes by comparing it with ionospheric data obtained from the local ionosonde, the IRI model, and daily solar activity indices.

EQIT-12 - Multi-static HF radar system in Peru - by Alexander Valdez Portocarrero

Status of First Author: Student IN poster competition, MS

Authors: David Hysell, Marco Milla, Ramiro Yanque, and Josemaría Gomez

Abstract: A multi-static HF radar system has been deployed in Peru to study the F-region in the equatorial sector. The main purpose of this system is to study the structure and dynamics of the bottom part of the F-region before the occurrence of a Spread-F event.

The current system has a transmitter station at the Ancon Observatory in Lima, Peru and 3 receiving stations: Ancón observatory, Huancayo Observatory (central part of Peru) and the third one at the Jicamarca Radio Observatory. The system transmits simultaneously two continuous wave radio signals at different frequencies: 2.72 and 3.64 MHz. The signals are modulated using PRN (Pseudo Random Noise) codes. Reflections from the ionosphere are collected at the different stations in order to determine the virtual heights corresponding to the different two frequencies. Using the information collected at the different stations, and applying a refraction tomography technique, we can invert a 3D plasma density distribution of the bottom part of the ionosphere in the central part of Peru, measurements that are important to understand the origin and evolution of the plasma irregularities.

In this work, we will first present a description of this multi-static radar which electronics is mainly based in Software Defined Radio (SDR) transceivers, specifically, on USRP2 devices. We will also present the current status of our database and the plans for expansion of the system.

IRREGULARITIES OF IONOSPHERE OR ATMOSPHERE

IRRI-01 - Characterization of Shortwave Fadeout seen in Daytime SuperDARN Ground-Scatter Observations - by Shibaji Chakraborty

Status of First Author: Student IN poster competition, PhD

Authors: S. Chakraborty, J. M. Ruohoniemi, and J.B.H. Baker.

Abstract: Shortwave fadeout (SWF) is one of the well-known radio wave anomalies that occur in the upper atmosphere. During a solar flare, the sun emits soft and hard X-rays in the order of ≤ 1 nm, which penetrate through the ionosphere and reach the D-layer, resulted in a sudden increase in plasma density. This sudden enhancement in plasma density increases the attenuation of radio waves. SWF causes disruption on HF communication channels that persists for 10's of minutes to a few hours. SuperDARN observations of daytime ground-scatter are strongly affected; the average number of ground-scatter echoes drops suddenly (≈ 1 min) and often reaches to zero. Ground-scatter echoes not only experience absorption but also undergo a sudden phase change [Watanabe et al. 2013] that leads to an apparent, brief increase in ground-scatter velocity, resulted in a 'velocity flash' feature. We have analyzed a number of events and report here on the characteristics of SWF in SuperDARN observations produced by M and X-class solar flares. The first effect of SWF is usually the velocity flash which lasts only a few 10s of seconds. Then the average number of ground-scatter echoes starts to decrease sharply marking an onset and leads to a blackout phase. During the blackout phase the ground-scatter is typically suppressed for 10s of minutes, and then it recovers back to pre-SWF echo-count through the recovery phase over half an hour. The intensity of SWF effect seen in SuperDARN ground-scatter depends on the solar zenith angle and operating frequency of the radar. In this presentation, we discuss the basic characteristics of SWF events seen in SuperDARN radar observations and different parameters which control the intensity of the event and the effect ionospheric dynamics during SWF. We also describe a Python-based tool that can monitor the ground-scatter observations and detects SWF across North America, using the network of SuperDARN radars.

IRRI-02 - Variations in equatorial spread F between conjugate sites - by Dustin Hickey

Status of First Author: Student NOT in poster competition, PhD

Authors: Carlos Martinis, Jeffrey Baumgardner, Michael Mendillo, and Joei Wroten

Abstract: Two Boston University all-sky imagers (ASI) in South America are well suited for studying inter-hemispheric differences of equatorial spread F. One imager is located in Villa de Leyva, Colombia (5.6° N, 73.5° W, 16.3° mag lat) and another is near the magnetic conjugate point in El Leoncito, Argentina (31.8° S, 69.3° W, -19.6° mag lat). We can measure the large scale (10s-100s km) plasma depletions in 630.0 nm airglow associated with ESF using these ASIs. Since large scale ESF is a flux tube aligned process, the depletions observed at these latitudes correspond to topside structures at the magnetic equator. We look at depletions occurring at both sites and find that in the majority of cases if depletions are present at one site, they are also present in the conjugate location at the same time. There are differences in the morphology and contrast of these depletions due to differences in magnetic field strength and thermospheric winds. To expand this project we also add GPS diagnostics to investigate the conjugate nature of smaller scale size irregularities associated with ESF. The results of this project will allow us to infer the conditions of the ionosphere at sites where local data is not available but instruments are located at the conjugate point.

IRRI-03 - On the Relationship between Sporadic-E and ENSO Observed by FORMOSAT-3/COSMIC - by Pei-yun Chiu

Status of First Author: Student IN poster competition, MS

Authors: Pei-yun Chiu¹, Loren Chang, Cornelius Csar Jude H. Salinas, Shih-Ping Chen, Yi Duann, Jann-Yenq Liu, and Charles Lin

Abstract: In recent years, many studies have shown evidence for several types of atmosphere-ionosphere coupling. In this study, we show the possible relation between Sporadic-E (Es) and El Nino-Southern Oscillation (ENSO) by using the FORMOSAT-3/COSMIC S4 scintillation index and tropopause height from 2007 to 2014. The long-term variation of the monthly midlatitudes median extreme S4 index in the E-region shows similar trend and periods in wavelet spectrum to ENSO. These results indicate that ENSO signatures can be transmitted to Es formation mechanisms, potentially through modulation of vertically propagating atmospheric tides that alter lower thermospheric wind shears.

IRRI-04 - First experiments at the (new) UAF-HAARP facility: preliminary artificial airglow results and guidelines for future experiments - by Christopher Fallen

Status of First Author: Non-student

Authors: Christopher T. Fallen, Brenton J. Watkins

Abstract: The High-frequency Active Auroral Research Program (HAARP) facility is the premier ionosphere radio modification facility for active space and radio science. Ownership of HAARP was transferred from DoD to the University of Alaska Fairbanks (UAF) in 2015 and is now managed by the Geophysical Institute (GI). UAF conducted its first HAARP experiment campaign in February 2017. The first campaign was funded by multiple sponsored PIs with varying independent research objectives. This poster describes airglow experiments conducted during the first UAF-HAARP campaign and offers suggested guidelines for proposing new funded experiments at the facility.

The primary ongoing objective of the airglow experiments described here is to measure white-light artificial airglow morphology with high time resolution simultaneously from HAARP and Poker Flat Research Range (PFRR). Specifically, spatiotemporal variation of airglow intensity from up-B and PFRR side views will be measured during experiments. The experiment modes and measurement techniques will

be used in conjunction with data gathered to resolve two specific science questions: 1) Is reported artificial airglow from X-mode HAARP experiments caused by X-mode polarized waves or instead by elliptical polarization that is not pure X-mode? 2) Do O-mode artificial airglow intensity variations vary with interaction altitudes relative to the 2nd electron gyro-harmonic as they varied with previous HF-enhanced ion-line and plasma-line intensity observed with the co-located (currently inoperable) AMISR-class UHF radar (MUIR) at HAARP?

While significant O-mode airglow was recorded with the Gakona all-sky camera on 22 February 2017 (AKST)—the fourth and final night of the campaign—variable thin high-level clouds present during the fourth-day experiment are insufficient to form conclusions based on airglow intensity data. No artificial airglow was measured during X-mode transmissions. Space and tropospheric weather variability, in combination with minor measurement equipment difficulties on the first day, prevented gathering of usable airglow data during the previous three experiment days. Factors outside of PI control such as geophysical conditions during a campaign are part of any active ionosphere experiment and some of these factors are unique to HAARP. Guidelines are suggested for planning and proposing funded space and radio science experiments at the UAF-HAARP Observatory.

IRRI-05 - In-situ and ground-based observations of equatorial plasma irregularities and implications for Spread F dynamics - by Dev Joshi

Status of First Author: Student IN poster competition, PhD

Authors: Dev Joshi, Keith Groves, John Retterer, Patrick A Roddy, and Chaosong Huang

Abstract: Equatorial Spread F is an important problem in space-aeronomy characterized by large-scale instabilities in the post-sunset low-latitude ionosphere and the subsequent formation of medium to small scale irregularities over large regions. These irregularities can cause severe space weather impacts in the form of deleterious radio wave scintillation effects on man-made technologies such as satellite communications and global navigation satellite systems (GNSS). The responsible mechanism for Spread F, formally identified as the gravitational Rayleigh-Taylor Instability, is commonly described as depletions or low density plasma “bubbles” that originate at the magnetic equator and expand poleward as the perturbation electric fields map along magnetic field lines. In this paradigm the meridional extent of the disturbances is wholly determined by the height of the bubbles at the equator. Here we present an investigation of the occurrence and altitudes of bubbles as a function of solar flux from in situ observations in the context of ground based scintillation measurements. We analyze electron density data from the Communication/Navigation Outage Forecasting System (C/NOFS) satellite developed by the Air Force Research Laboratory and launched into an elliptical low earth orbit at an inclination of 13° , a perigee of 400 km and an apogee of 850 km. While the altitude variation of the spacecraft complicates the statistical comparisons of parameters for purposes that require height-normalized values, it readily supports investigations of altitude variability, specifically electron density irregularities. The investigation presented here will identify the regions affected by low-latitude scintillation, enhance our ability to model radio occultation results and provide insight into the growth mechanism and longitudinal variability of equatorial spread F. We present the first ever extensive comparison between ground station scintillation observations and satellite observations of the ion density irregularities. This may provide new insight into the flux-tube expansion mechanism of equatorial plasma bubbles. Moreover, the space-based platform supports an analysis of longitudinal variations in spread F occurrence.

IRRI-06 - A Global Study of Ionospheric Irregularities during Daytime at the Magnetic Dip Equator using SCINDA Ground-based and Radio Occultation Measurements - by Aramesh Seif

Status of First Author: Non-student

Authors: Aramesh Seif, Jann Yenq Liu

Abstract: Ionospheric scintillations at gigahertz (GHz) frequencies have been observed during both day and night. For the most part, scintillations have been found to be associated with the F layer at night and with sporadic E (Es) layer during the day. The basis for the association of radio scintillations to Es is largely observational. Given that this association appears to be real, researchers have invoked the wind-shear theory as its source mechanism. This theory was proposed for the mid-latitude ionosphere, where the inclination of the geomagnetic field (B) is steep enough to produce a thin layer of high plasma density, via the wind-shear theory. The plasma density supposedly becomes high enough, and its gradient becomes steep enough, so that the geometry would seem to be unstable, in the presence of a background neutral wind, to the gradient-drift process. Nevertheless, this theory fails to operate at the magnetic dip equator, where inclination of the B is very small or even zero. This implies that B must have a significant inclination angle; therefore, we do not expect the presence of Es at the magnetic dip equator. In other words, theoretically daytime scintillation activities would not be expected in the vicinity of the magnetic dip equator; however, our results showed the daytime scintillation occurred near the magnetic dip equator. Therefore, the key objective of this study is to further improve our understanding as to what is the physical process responsible for the formation of these scintillation patches. To answer this question, we study the global characteristics of daytime GHz scintillation in association with the Es phenomena to understand where and how the Es patches do form in this region. Our understanding of both phenomena could be improved by acquiring a better understanding of either phenomenon.

This study focuses on the detection and analysis of Es from RO measurements, to conclusively show the presence of Es's relationship with daytime scintillation. We bring two data sets to bear, using the Global Navigation Satellite System (GNSS) signal transmissions received on the ground and from space, which provide a unique opportunity to retrieve information about Es. Hence, complementary information is available regarding plasma structure in an Es patch. An analysis of combined data sets should prove to be a profitable avenue for research. In this study, we present the occurrence of daytime scintillation from the Scintillation Network Decision Aid (SCINDA) GPS ground-based receivers using six stations situated very close to the magnetic dip equator. To better understand scale size irregularities as well as identify the occurrence of Es, we use COSMIC RO data. Two key findings coming out from our study are (1) according to the characteristics of daytime GHz scintillation analyzed at SCINDA station, strong daytime GHz scintillation observed near the dip equator. (2) The results obtained from GNSS RO measurements provide information on the existence of altitude and intensity of electron density irregularities at ionospheric E region height. This indicates that Es is associated with daytime GHz scintillation.

IRRI-07 - Reconstruction of the GPS phase scintillation during a magnetospheric substorm - by Sebastijan Mrak

Status of First Author: Student IN poster competition, PhD

Authors: Sebastijan Mrak, Joshua Semeter

Abstract: Auroral particle precipitation during a geomagnetic substorm release vast amount of free energy in the Earth's ionosphere, causing an impact ionization and secondary plasma irregularities producing L-band phase scintillation. The Mahali Global Positioning System (GPS) 9-receiver array deployed in central Alaska, has probed a sequence of Westward Traveling Surges (WTS) in magnetic field line direction with a ~ 15 -km baseline distance. We present a case study of GPS phase scintillation reconstruction, for the geomagnetic substorm on October-07, 2017, using data from GPS receivers, All-Sky Imager (ASI) and the Poker Flat Incoherent Scatter Radar (PFISR). First, GPS observations are merged with green line (557.7-nm) emissions, mapped to an estimated altitude of 120-km, to spatially associate phase scintillation and optical emissions. Then, PFISR derived plasma electron density profiles from several GPS-PFISR co-aligned beams are included in the reconstruction study to constrain the altitude of scintillation producing irregularities. Combined data from the dense receiver array show that phase scintillation happen both, during substorm's expansion and recovery phases. GPS-ASI merged study reveals that most intense scintillation is found in the trailing edge of auroral arcs. Lastly, co-aligned PFISR observations constrain the altitude of the scintillation producing irregularities to the E-region (100-km--150-km).

IRRI-08 - Detection of Spread-F, foF2 values and Planetary and Gravity Wave Signatures using Digisonde and VIPIR instruments and their comparison with COSMIC-1/FORMOSAT-3 data - by Preeti Bhaneja

Status of First Author: Student NOT in poster competition, PhD

Authors: Preeti Bhaneja

Abstract: This research involves a case study of Midlatitude Spread F (MSF) at Wallops Island (37.8°N, 75.5°W) using digisonde and VIPIR data. Various algorithms have been written to process the raw data and determine spread F by using edge detection and pattern recognition techniques. Algorithms have also been written to find foF2 and hmF2 values for obtaining the density profile of the ionosphere. We have also included results from five midlatitude stations in north-America. Findings based on work carried out to date include:

1. Determination of seasonal and solar cycle variation patterns of MSF.
2. The results obtained are compared with manually scaled ionograms using the Standard Archiving Output (SAO) software created by Lowell to determine the accuracy of the algorithms.
3. Correlation between digisonde, VIPIR and COSMIC-1/FORMOSAT-3 satellite data values to check for discrepancies and validity of data.
4. Wave analysis has been performed to detect the presence of planetary and gravity wave patterns in foF2 values with periods ranging from a few hours to a few days and also for various seasons.

IRRI-09 - Equatorial Plasma Bubbles: variations of occurrence and spatial scale in local time, longitude, season and solar activity - by Jonathon Smith

Status of First Author: Student IN poster competition, PhD

Authors: Jonathon Smith, Roderick Heelis

Abstract: We examine the location and structure of equatorial topside depletions referred to here as equatorial plasma bubbles (EPB). The Coupled Ion Neutral Dynamics Investigation (CINDI) Ion Velocity Meter (IVM) instrument onboard the Communication/Navigation Outage Forecasting System is used to measure the ion density from August 2008 to December 2014, a time period in which solar activity transitioned from solar minimum conditions to more moderate solar activity conditions. EPB data is divided into four longitude sectors to determine seasonal and solar cycle variability. In the early phase of the mission, during solar minimum, EPB occur late in local time, primarily after midnight in all longitude sectors. In the later phase of the mission EPB occurrence after midnight diminishes in all seasons and longitude sectors with the exception of the sector extending from -15° to 60° . An examination of the widths of bubbles indicates that all longitudes show similar distributions between 115 km and 460 km with a prominent peak near 200 km. Among these widths is a distinct width that belongs to discrete individual bubbles with no sub-structure. We suggest that many bubbles are actually combinations of these individual bubbles, however in the later phase of the mission there is a population of bubbles that do not conform to this description; perhaps due to the influence of large-scale plasma motions affecting the background density in which they are embedded.

IRRI-10 - Deployable Satellite Receiver Node Design to Measure Ionospheric Scintillation - by Xiaoyu Han

Status of First Author: Student NOT in poster competition, BS

Authors: Han, Xiaoyu Brosie, Kayla Leffke, and Zachary Earle, Gregory

Abstract: On August 21, 2017, there will be a solar eclipse over the United States traveling from Oregon to South Carolina. It offers a unique opportunity to study ionospheric scintillation that may occur during the

eclipse. To obtain a comprehensive understanding of scintillation, there will be three receiver nodes deployed at three different locations over the continent. The sites will receive signals from Inmarsat 4F3 at a known beacon frequency, along three different lines of sight. In addition, signals from known low earth orbit (LEO) satellites will also be utilized if they provide line of sight paths through the ionosphere. The receivers are designed to be compact and user friendly for ease of transportation and assembly. They will measure fluctuations of the received satellite signals during the eclipse and compare them to fluctuation levels measured during normal conditions. The objectives of this research are to create an affordable ground receiver design to measure ionospheric scintillation that can be easily deployed during the eclipse. The receiver consists of inexpensive software defined radios (SDR), small scale antennas, and open source software. The deployment locations are chosen to have a line of sight to the satellites that pass through the eclipsed region. The receiver nodes may be relocated to local high schools for educational purposes and operated remotely via internet to routinely monitor the ionosphere after the eclipse experiment. This poster will describe the antenna and SDR systems, and show observations made in Blacksburg, Virginia in 2017.

IRRI-11 - Sensing Ionospheric Irregularities with a GNSS Receiver Array during a Geomagnetic Storm - by Yang Su

Status of First Author: Student IN poster competition, PhD

Authors: Yang Su, Seebany Datta-Barua, Gary Bust, and Kshitija Deshpande

Abstract: Carbon dioxide (CO₂) is an important greenhouse gas that characterizes the energetics and dynamics of the stratosphere and mesosphere. Distributions of the CO₂ volume mixing ratios (VMR) in the stratosphere (from 30 up to ~ 60 km) have been derived from Solar Occultation for Ice Experiment (SOFIE) onboard the Aeronomy of Ice in the Mesosphere (AIM) satellite from the 4.3 μm band. This is the first time that the CO₂ VMR has been retrieved from space in the 30-60 km altitude range. The data set spans from April 2007 to current date. The retrieval of CO₂ is performed by using a non-local thermodynamic equilibrium (non-LTE) retrieval scheme and refraction derived temperature. In this paper we present preliminary results of SOFIE CO₂ VMR time series and seasonal variation. The agreement between the SOFIE CO₂ trend and Mauna Loa surface measurement suggests that the retrieval algorithm is reliable. Annual average of seasonal variation is compared with simulations using the Specified Dynamics version of the Whole Atmosphere Community Climate (SD-WACCM). The CO₂ distribution is driven by the general circulation, descending or ascending in the summer (August to October in Northern Hemisphere and March to May in Southern Hemisphere) polar region, but only diverging in winter (July, August and September) in Southern Hemisphere. In addition, there is a weaker peak in winter Northern Hemisphere. Stratospheric sudden warming (SSW) causes strong CO₂ variation. During a major SSW the polar vortex is almost entirely broken down and vertical transport even the Cross-Tropopause Flux is stronger. At last, we report the variation of CO₂ VMR and temperature after two SSW events in 2009 and 2013, and discuss about the dynamical mechanisms with the help of SD-WACCM.

IRRI-12 - Radar Imaging with MaxEnt for Manastash Ridge Radar - by Marcos Inonan

Status of First Author: Student NOT in poster competition, BS

Authors: Marcos Inonan, John D. Sahr

Abstract: The Manastash Ridge Radar (MRR) is a passive radar that observes ionospheric field-aligned irregularities by detecting the scatter of commercial FM radio broadcasts. We have used the MaxEnt spectral analysis method to apply image reconstruction in spaced antenna receivers. Currently, MRR has three independent data points that permits to produce fine azimuthal structure of field-aligned irregularities in the high-latitude E region ionosphere

IRRI-13 - June solstice equatorial spread F: On the role of weak vertical plasma drifts - by Weijia Zhan

Status of First Author: Student IN poster competition, PhD

Authors: Weijia Zhan, Fabiano S. Rodrigues, and Marco A. Milla

Abstract: Equatorial spread F is the name given to signatures of ionospheric irregularities, produced in various types of instruments, and commonly observed after sunset hours at low magnetic latitudes.

ESF has high occurrence rates, in most longitude sectors, during equinox months. This has been associated with the expected high value of the ExB vertical plasma drifts driven by the pre-reversal enhancement (PRE) of the equatorial zonal electric field. The vertical plasma drift is considered the main parameter controlling the development of interchange plasma instabilities responsible for ESF. During June solstice, however, the PRE is severely reduced specially during low solar flux conditions. Late-night ESF events have been reported, nevertheless, during those conditions.

It has been hypothesized that late-night weak vertical plasma drifts can still produce conditions favorable to the development of plasma instabilities leading to ESF. In this study, we conducted a careful analyses of incoherent and coherent scatter radar observations of ionospheric drifts and ESF made at the Jicamarca Radio Observatory. We present experimental evidence of the development of June solstice ESF under weak vertical plasma drift conditions. Numerical analyses are also presented in support of the observations.

IRRI-14 - Zonal Structure in All Sky Images of Auroral Features - by Robert Finan

Status of First Author: Student NOT in poster competition, BA

Authors: Robert Finan, Michael Mendillo, Carlos Martinis, Jeff Baumgardner, and Joei Wroten

Abstract: The BU imaging group collects data using All Sky Imagers (ASI) placed around the globe, which detect emissions from the upper atmosphere at various wavelengths of light. In this work I present results showing Stable Auroral Red (SAR) Arcs that occur at sub-auroral latitudes and observed in 6300Å. This emission arises from atomic oxygen via collisions with thermally energetic electrons in the Earth's upper atmosphere. ASI's show that typical SAR Arcs are narrow (~ 2° latitude), uniform arcs, and typically monochromatic. Here I describe a SAR arc observed on October 2, 2013 at Millstone Hill (42.6N, 71.5 W, 52.2N (mag.)) with several superimposed patches of emission in two oxygen lines, 6300 Å and 5577 Å. I demonstrate that the red and green line emissions come from the same height domain (350–400 km). Seven brightness peaks with average longitude spacing of ~4° are clearly observed. Observations of total electron content (TEC) from GPS satellites showed increases in TEC and signal phase fluctuations when the raypaths crossed one of the optical features. A plausible explanation of all four effects (red and green optical emissions, increases in TEC, and radiowave scintillations) points to the presence of low-energy (<100 eV) electron precipitation. Similar beaded structures are observed in 6300A at the magnetically conjugate site in Rothera (67.6S, 68.1W, 57.7S (mag.)).

LONG TERM VARIATIONS OF THE IONOSPHERE-THERMOSPHERE

LTVI-01 - Observed increase in geocoronal hydrogen emissions - by Susan Nossal

Status of First Author: Non-student

Authors: Susan Nossal, Edwin Mierkiewicz, Fred Roesler, R. Carey Woodward, Derek Gardner

Abstract: There is evidence for an observed increase in the WI Northern hemisphere hydrogen emission data set between two successive solar maxima periods of solar cycles 22 and 23, but not between solar

minimum periods. This increase has not been explained by calibration, tropospheric scattering, data analysis approaches, modeling of the effects of greenhouse gases or our understanding of the effect of the solar cycle variation on hydrogen emissions. We will discuss the observations in the context of knowledge of the diurnal, solar cyclic, and climatic influences on geocoronal hydrogen and connections to hydrogen species below.

LTVI-02 - Diurnal variation of atomic hydrogen density in the terrestrial upper atmosphere - by Yamuna Phal

Status of First Author: Student IN poster competition, PhD

Authors: Yamuna Phal, Lara Waldrop, Jianqi Qin, and Larry Paxton

Abstract: Accurate quantification of the abundance and spatial distribution of the atomic hydrogen (H) population in the terrestrial atmosphere is critical for many disparate investigations in aeronomy and magnetospheric physics, including MLT chemistry and energetics, thermosphere/ionosphere coupling, long-term atmospheric evolution, and energy dissipation in the ring current following geomagnetic storms. However, current understanding of this key species is based mainly on theoretical and numerical models and their heavy reliance on fundamental assumptions of thermospheric and exospheric conditions that have never been validated due to the long-standing sparseness of H density measurements. Our recent development of a sophisticated radiative transport model enables the reliable interpretation of remotely-sensed measurements of optically-thick H emission, such as those acquired along the Earth's limb and disk by the Global Ultraviolet Imager (GUVI) onboard NASA's Thermosphere Ionosphere Mesosphere Energetics and Dynamics (TIMED) spacecraft from 2002-2007. In this work, we present results from our investigation of variations of the brightness of emission at 121.6 nm (Lyman-alpha) along the Earth's dayside limb, which we use to derive the atomic hydrogen density distribution from ~250 km out to ~1 Re. GUVI's unprecedented spatial and temporal coverage of this atmospheric layer allows for the first unambiguous characterization of diurnal variation in H density near and above the nominal exobase. Our results reveal stark differences in the local time variations in H density between high and low altitudes, which are indicative of large scale structure possibly relating to both thermally-driven outflow as well as non-thermal forcing.

LTVI-03 - Spectral Analysis of the Neutral Wind Components over Arecibo based on Five Consecutive Years (2012-2017) of Fabry-Perot Observations - by Eframir Franco-Diaz

Status of First Author: Non-student

Authors: Eframir Franco-Diaz, Christiano G.M. Brum and Robert B. Kerr

Abstract: The Fabry-Perot Interferometer (FPI) localized at the Arecibo Observatory has been monitoring the upper meridional and zonal thermospheric winds components since 1989. A few years ago, an upgrade was completed, enabling it to do automatic Doppler Imaging measurements of the neutral atmosphere dynamic on a nightly basis while the weather permitted it. This work presents thermospheric neutral winds (TNW) day-to-day variability in the mid-latitude upper atmosphere based on FPI observations from May 29, 2012 to April 30, 2017. Our approach for this study consists of a spectral analysis of the TNW component residual obtained from the difference between the data and an empirical model based on the data itself (for low geomagnetic activity and solar condition taking into account the season and local time dependencies). For the spectral analysis, we applied the wavelet transform technique using the orthonormal discrete Meyer wavelet mother function (the signal was decomposed in nine (9) orthogonal frequency levels). Several patterns were identified in the different levels of decomposition, but the most intriguing one was detected in the D7 level (128-256 days) which showed a strong seasonal dependence of phase progression for both of the TNW components, but not similar local time modulation. However, when the computed vertical neutral wind (W) for the D7 decomposition level (based on the horizontal TNW components) was retrieved, a clear influence of W on the horizontal components was detected.

LTVI-04 - The long-term trends in thermospheric mass density and ionospheric total electron content - by Rong Tsai-Lin

Status of First Author: Student IN poster competition, MS

Authors: Rong Tsai-Lin, Jack C. Wang, Loren C. Chang, Huixin Liu, and Charles Lin

Abstract: In this research, we present spectral analysis of the daily thermospheric total mass density derived from ~5000 near-Earth space objects from 1967 to 2012 [Emmert et al., 2004; Emmert et al., 2008], as well as GPS total electron content from 1995 - 2012. In our analysis, we consider the roles played by solar and geomagnetic activity, as well as possible coupling to the stratospheric quasi-biennial oscillation (QBO), the El Nino Southern Oscillation (ENSO), and the manifestation of possible ionosphere / thermosphere coupling.

MIDLATITUDE THERMOSPHERE OR IONOSPHERE

MDIT-01 - Wind Field Plotting for Red and Green Line Scanning Doppler Imager Data - by Kylee Branning

Status of First Author: Student IN poster competition, PhD

Authors: Kylee Branning, Mark Conde

Abstract: Using Scanning Doppler Imagers (SDI), we are able to map winds and temperatures across a region of sky visible from a ground-based site. Despite the 558 nm green line being brighter in the auroral zone, most SDI applications have made use of the bright 630 nm red line data because of its simplicity and its reliability as an indicator of middle thermospheric (F-region) conditions. Changing characteristic energy of the electron precipitation means that the green line height can vary anywhere in the range from 100-150 km altitude. This makes the data much harder to use since these variations commonly occur across the SDI field of view. This height range is a region where strong vertical gradients are the norm, so combining data from different look directions across the sky often means combined measurements of different wind fields leading to meaningless results. However, using temperature skymaps we can estimate the emission height; therefore, we know whether strong height variations have occurred. Apart from local times in the pre-midnight sector, strong height variations across our field of view are not all that common which means there are many times when we can measure the wind field without a problem. Nevertheless, if strong height variations do occur, we can exploit them over a time window of approximately 30-60 minutes to measure the height variation of the wind. Looking through the data we can find times when the green line winds are likely good, and we can compare these with the F-region winds from higher up. We can use this approach to probe how ion-drag forcing penetrates down into the E-region. Examples will be presented in the poster.

MDIT-02 - Arecibo Observatory - HF facility and diagnostics - by Eliana Nossa

Status of First Author: Non-student

Authors: Christiano Brum, Mike Sulzer, Alfredo Santoni, and Phil Perillat

Abstract: The Arecibo Observatory has an HF facility that allows ionospheric modification experiments. The HF facility works at a maximum of 600kW at two frequencies (5.1MHz and 8.175MHz). The diagnostics of the ionospheric enhancements are made by the sensitive Arecibo ISR and other extensive instrumentation that includes lidars, passive optics, other RF systems and more. Technical aspects of the facility are presented as well as samples of the diagnostic possibilities the Observatory allows.

MDIT-03 - Ionosonde-Based Indices for Improved Representation of Solar Cycle Variation in the International Reference Ionosphere Model - by Steven Brown

Status of First Author: Student IN poster competition, PhD

Authors: Dieter Bilitza, Erdal Yiğit

Abstract: A new monthly ionospheric index, IGNS, is presented to improve the representation of the solar cycle variation of the ionospheric F2 peak plasma frequency, foF2. IGNS is calculated using a methodology similar to the construction of the "global effective sunspot number", IG, given by Liu et al. (1983) but selects ionosonde observations based on Hemispheres. We incorporated the updated index into the International Reference Ionosphere (IRI) model and compared the foF2 model predictions with global ionospheric observations. We also investigated the influence of the underlying foF2 model on the IG index. IRI has two options for foF2 specification, the CCIR-66 and URSI-88 foF2 models. For the first time, we have calculated IG using URSI-88 and assessed the impact on model predictions. Results show that the inclusion of the new monthly IGNS index in place of the current 12-month smoothed IG index reduce the foF2 model prediction errors up to 50%. This is due to an overall improved prediction of foF2 seasonal and solar cycle variations in the different hemispheres.

MDIT-04 - The Arecibo Observatory Remote Optical Facility (AO-ROF) in Culebra Island, Puerto Rico: Current Status and Future Projects - by Pedrina Santos

Status of First Author: Non-student

Authors: Dr. Christiano Garnett M. Brum, Ms. Eva Roble

Abstract: The Arecibo Observatory (AO) Remote Optical Facility (ROF) is located ~ 95 miles East from AO (18, 3°N; 65, 3°W) in a reclusive and safe area of the island of Culebra, Puerto Rico. The AO-ROF is established since November 2015 and provides an economical opportunity to offer a superior data product to our scientific community and users. The idea of launching the AO-ROF was a solution to mitigate the ever cumulative quantity of cloud, fog, and rain that has distressed observations at the AO during major optical campaigns and observations. Given Culebra Island's favorable geographical and climatological characteristics as its low elevation and geographic location, it has more steady weather conditions than Arecibo, so therefore it provides more availability for optical observations. In addition, placed on Culebra, optical instruments can observe the same thermospheric volume over AO sampled by the Incoherent Scatter Radar (ISR). This capability became especially important during the High Frequency (HF) campaigns, run by the new AO Heating Facility. In this work we present an overview of the current status of the AO-ROF and future projects.

MDIT-05 - O-O+ momentum imbalance in the topside ionosphere: implications for bias in MSIS oxygen density specification - by Pratik Joshi

Status of First Author: Student IN poster competition, PhD

Authors: P. Joshi, L. Waldrop, C. Brum, M. Sulzer, N. Aponte, S. Gonzalez, P. Santos and E. Robles

Abstract: A long-standing uncertainty in ionosphere/thermosphere model formulation concerns the specification of the cross section for resonant charge exchange between neutral atomic and ionized oxygen, O and O+, the principle constituents between ~ 200 – 500 km in the terrestrial atmosphere. O–O+ charge exchange plays a vital role in both momentum and energy exchange between the thermosphere and ionosphere, such that the value of the cross section, $Q(O-O^+)$, strongly influences calculations of plasma drift speeds, diffusion coefficients, and electron density distributions. No direct measurement of $Q(O-O^+)$ exists at the thermal energies characteristic of the upper atmosphere, and many physics-based model formulations often incorporate the notorious "Burnside factor" scaling, typically ranging from 1.3–1.7, to allow for user adjustment of this fundamental parameter. Parametric constraint of O+ momentum balance

has been used for decades to interpret discrepancies between observation and theory in terms of the unknown Burnside factor. The long-standing lack of reliable [O] specification, however, introduces an ambiguity regarding the physical meaning of this “correction” factor: while it is usually intended to constrain theoretical estimates of $Q(O-O^+)$, it could also reflect systematic bias in the required model specification of [O] for momentum balance analysis. In this work, we revisit O^+ momentum balance and its implications for potential bias in the NRLMSISE-00 thermospheric density model in particular through our analysis of an unprecedented baseline of combined incoherent scatter radar and neutral wind data acquired at Arecibo Observatory from 1984-2004. While a statistically significant non-unity average Burnside factor is observed, the analysis also reveals clear and consistent local time, seasonal, and solar activity trends which we interpret as compelling, though not conclusive, evidence for thermospheric model bias, a result itself which has wide-reaching implications for aeronautical studies.

MDIT-06 - Statistical Study of Nightside Quiet Time Subauroral Ionospheric Convection Observed by the North American Midlatitude SuperDARN Radars - by Maimaitirebike Maimaiti

Status of First Author: Student IN poster competition, PhD

Authors: M. Maimaiti (1), J. M. Ruohoniemi (1), J. B. H. Baker (1), and A.J. Ribeiro (1)

1. Department of Electrical and computer Engineering, Virginia Tech, Blacksburg, VA, USA

Abstract: Studies have shown that ionospheric plasma in the subauroral region exhibits drifts of a few tens of m/s under quiet time conditions. However, the exact driving mechanisms for the low velocity subauroral plasma motion are not well understood. The recent expansion of SuperDARN radars to the midlatitude regions has provided opportunities to study subauroral ionospheric convection over large areas and with greater resolution and statistical significance than previously possible. The radars frequently observe subauroral ionospheric backscatters with low doppler velocities on most geomagnetically quiet nights. In this study we have taken two years of quiet-time nightside data from six midlatitude SuperDARN radars in the U.S. continent to derive a statistical model of mid-latitude plasma convection between 52° - 58° magnetic latitudes. The model is organized in MLAT-MLT coordinates and has a spatial resolution of $1^{\circ} \times 7$ min with each grid having > 5000 contributing measurements on average. Our results show that the flow is predominantly westward (20 - 40 m/s) and weakly northward (0 -10 m/s) deep in the nightside. The convection is greatly affected by season, with the flows being strongest and most variable in winter. The statistical results presented here are in basic agreement with previously reported observations from ISR measurements but also show new features. One such feature is a significant latitudinal variation of zonal flow velocity near midnight in winter. In this presentation, we describe the derivation of the nightside quiet-time subauroral convection model, examine the most prominent features and discuss the results in terms of possible mechanisms.

MDIT-07 - Longitudinal structure in electron density at mid-latitudes: upward-propagating tidal effects - by Kedeng Zhang

Status of First Author: Student IN poster competition, PhD

Authors: Hui Wang and Kedeng Zhang

Abstract: This work studies the upward-propagating migrating and non-migrating tidal effects from the lower atmosphere on the longitudinal variation of electron density (ΔN_e) in both E and F regions at mid-latitudes during the 2002 March equinox. A total of 12 runs are conducted using Thermosphere Ionosphere Electrodynamic General Circulation model (TIEGCM) for theoretical investigation. The ΔN_e at altitudes above 200 km is affected by upward propagating tides, with maximum values attained around 300 km. Migrating tides result in reduced longitudinal differences in the ΔN_e over North America (NA) and in

the Southern Hemisphere, while non-migrating tides induce a wave-4 pattern in both hemispheres. The non-migrating effect is weaker than migrating effect after penetrating into F region. The neutral composition (i.e. ratio between atom oxygen and molecular nitrogen) is dominant in regulating ΔNe in both the migrating (accounting for approximately 64%) and non-migrating (about 60%) tidal penetration process. The ΔNe caused by the tidal meridional wind (accounting for approximately 70%) is stronger than the tidal zonal wind (about 30%) under both migrating and nonmigrating tidal conditions, except in the Southern Hemisphere under migrating tidal input. This work contributes to our understanding of the mechanisms for the longitudinal modulation of ΔNe at mid-latitudes.

MDIT-08 - Helium Structure in the Upper Thermosphere - by Torfinn Johnsrud

Status of First Author: Student IN poster competition,

Authors: Torfinn Johnsrud, Dr. Jeffrey P. Thayer

Abstract: Helium is an important contributor to mass density behavior in the upper thermosphere. Its distribution is influenced by winds and diffusion as it transitions from a minor species in the lower thermosphere to a major species in the upper thermosphere. Because of its influence on mass density and the drag coefficient on spacecraft, helium behavior influences the drag force on spacecraft. This poster will exercise the NCAR-TIEGCM V2.0, which includes helium as a major species, and the NRLMSIS-00 model to evaluate simulations of helium structure in the upper thermosphere.

MDIT-09 - Seeking Lagrangian Coherent Structures in Ionospheric Plasma Drift Flows - by Ningchao Wang

Status of First Author: Student IN poster competition, PhD

Authors: Ningchao Wang, Uriel Ramirez, and Seebany Datta-Barua

Abstract: Lagrangian Coherent Structures (LCSs) is a numerical technique in fluid dynamical analysis predicting transport and interaction processes. LCSs are frame-invariant structures independent of the observer [1] describing the maximum separation (or convergence) regions in the flow [2]. LCSs are found and illustrated in the thermosphere. Previous work showed that the global thermospheric LCSs are more prominent at higher altitudes and latitudes, and respond to geomagnetic activity [3]. In this work, we apply the LCS technique to an ionospheric model to explore the LCSs in plasma drift flows. The most commonly used computational method for finding LCSs is to compute the finite time Lyapunov exponent (FTLE), a scalar field measuring the ratio of stretching after a given interval of time among neighboring particles, relative to their initial separation. LCS ridges are located at the local maxima of the FTLE. A 2D algorithm, Ionosphere-Thermosphere Algorithm for Lagrangian Coherent Structures (ITALCS), is used for computing the forward-time FTLE scalar fields in the ionospheric drift field to visualize the ionospheric LCSs. For the initial study, the ionosphere is treated as a 2D closed spherical domain and discretized in longitude and latitude. The Weimer 2005 [4] polar electric potential model and the 12th generation International Geomagnetic Reference Field [5] are used to generate the ExB drift field at each grid point in the ionosphere. The ExB drifts are used as the input to ITALCS. The ionospheric LCSs are found at middle to high latitudes for both geomagnetically quiet period, 0 UT 17th March 2015, and geomagnetically active period, 12 UT 17th March 2015. During the geomagnetically stormy period, LCSs become more complex and move equatorward in both northern and southern hemispheres compared to the quiet time LCSs. The ionospheric LCSs responding to geomagnetic activity agrees with the thermospheric LCSs discussed in [3]. This agreement indicates that the LCSs technique could be used to analyze energy exchange and transport in the ionosphere-thermosphere system.

References

I. G. Haller, "An objective definition of a vortex," *Journal of Fluid Mechanics*, 525, 2005, 1-26, doi: <https://doi.org/10.1017/S0022112004002526>.

2. G. Haller, "Lagrangian coherent structures," *Annual Review of Fluid Mechanics*, 47, 2015, 137–162, doi:10.1146/annurev-fluid-010313-141322.
3. N. Wang et al., "Lagrangian Coherent Structures predict transport in the thermosphere," *Geophysical Research Letters*, accepted.
4. D. R. Weimer, "Predicting Surface Geomagnetic Variations Using Ionospheric Electrodynamical Models," *J. Geophys. Res.*, 110, 2005, doi:10.1029/2005JA011270.
5. E. Thébault et al., "International geomagnetic reference field: the 12th generation," *Earth, Planets and Space*, 67.1, 2015, 1-19, doi: 10.1186/s40623-015-0228-9.

MAGNETOSPHERE-IONOSPHERE-THERMOSPHERE COUPLING

MITC-01 - Model-data comparison of neutral wind impacts on high-latitude ionospheric upflows - by Meghan Burleigh

Status of First Author: Student IN poster competition, PhD

Authors: M. Burleigh, M. Zettergren, C. Heale, and J. Snively

Abstract: Several different physical processes are known to contribute to escape of ionospheric plasma into the magnetosphere at auroral latitudes. Soft electron precipitation and strong DC electric fields heat the ambient electron and ion populations leading to expansion and upflow in the F-region, while gyro-resonant transverse plasma waves in the topside ionosphere can accelerate ions above escape energy. Thermospheric winds are known to play a strong role in regulating ionospheric dynamics in the E- and F-region ionosphere, but have not been fully examined as a source of ion upflow that may contribute to escape. Winds can impact high-latitude ion upflows through the regulation of ion densities and momentum in the F-region. Few detailed observational or modeling studies have been devoted to these interactions. In this work we use an anisotropic fluid model of the ionosphere to examine how neutral winds may drive ion upflows. This model is based on a Bi-Maxwellian distribution for the ions and solves time-dependent, nonlinear equations of conservation of mass, momentum, parallel energy, and perpendicular energy for species important to E-, F-, and topside ionospheric regions. It includes chemical and collisional interactions with the neutral atmosphere and a perpendicular energy source term to encapsulate ion energization by transverse plasma waves. This ionosphere model is coupled to a neutral dynamics model to analyze several instances found in Sondrestrom incoherent scatter radar data where winds from atmospheric gravity waves appear to play a role in modulating ion upflows. Model-data comparisons suggest the presence of large amplitude gravity waves capable of impacting parallel ion transport and provide some indication of the processes that may be responsible for these waves as well as the wave dynamics affecting upflow. Simulations and data analysis illustrate the detailed physical processes by which the waves impact ion density and transport and suggest a role for neutral dynamics in the ion escape process.

MITC-02 - Magnetosphere-ionosphere-thermosphere coupling through H redistribution driven by geomagnetic storms - by Jianqi Qin

Status of First Author: Non-student

Authors: Jianqi Qin, Lara Waldrop, and Jonathan J. Makela

Abstract: Atomic hydrogen (H) is the dominant neutral constituent in the terrestrial upper atmosphere and plays a critical role in coupling the thermosphere-ionosphere system to the magnetosphere and solar wind through ion-neutral interactions. These coupling effects can manifest as evident changes in the geocorona H emissions during storm times. In this study, geocoronal H emission data acquired by the Global Ultraviolet Imager (GUVI) onboard NASA's Thermosphere Ionosphere Mesosphere Energetics and Dynamics (TIMED) mission are analyzed to quantify the H density distribution over the entire magnetosphere-

ionosphere-thermosphere region in order to investigate the response of the atmospheric system as a whole to geomagnetic storms. A comprehensive radiative transfer model is used in the H density quantification. Through the analysis of over 20 storm events, we find that the storm-time H density in the lower thermosphere and upper exosphere increases, while the H density in the transition region decreases relative to the density values at quiet times. The H depletion in the transition region tends to be less significant for weaker storms that are analyzed in this study. We propose that enhanced ion-neutral interaction in the topside ionosphere and inner plasmasphere might be the primary driver of the storm-induced vertical H redistribution, and that contributions from vertical transport of the H atoms might have also been involved. The resulting enhanced hot H- and O-atom precipitation from the topside ionosphere and inner plasmasphere might be partially responsible for the storm-time enhancements in the thermospheric ultraviolet airglow emissions documented in the literature. Although our quantification can only reveal vertical H redistribution, we suspect that lateral H redistribution might also occur during storm times. We emphasize that H redistribution should be considered as an important process in the study of storm-time atmospheric evolution.

MITC-03 - On the relation between soft electron precipitations in the cusp 1 region and solar wind coupling functions - by Tong Dang

Status of First Author: Student IN poster competition, PhD

Authors: Tong Dang, Binzheng Zhang, Michael Wiltberger, Wenbin Wang, Xiankang Dou, Weixing Wan and Jiuhou Lei

Abstract: In this study, the correlations between the fluxes of precipitating soft electrons in the cusp region and solar wind coupling functions are investigated utilizing the Lyon-Fedder-Mobarry (LFM) global magnetosphere model simulations. We conduct two simulation runs during periods from 20 March 2008 to 16 April 2008 and from 15 December 2014 to 24 December 2014, which are referred as “Equinox Case” and “Solstice Case”, respectively. The simulation results of “Equinox Case” show that the plasma number density in the high-latitude cusp region scales well with the solar wind number density ($n_{\text{cusp}}/n_{\text{sw}}=0.78$), which agrees well with the statistical results from the Polar spacecraft measurements. For the “Solstice Case”, the plasma number density of high latitude cusp in both hemispheres increases approximately linearly with upstream solar wind number density with prominent hemispheric asymmetry. Due to the dipole tilt effect, the average number density ratio $n_{\text{cusp}}/n_{\text{sw}}$ in the Southern (summer) Hemisphere is 0.55 larger than that in the Northern (winter) hemisphere. In addition to the solar wind number density, twenty solar wind coupling functions are tested for the linear correlation with the fluxes of precipitating cusp soft electrons. The statistical results indicate that the solar wind dynamic pressure p exhibits the highest linear correlation with the cusp electron fluxes for both equinox and solstice conditions, with correlation coefficients greater than 0.75. The linear regression relations for equinox and solstice cases may provide an empirical calculation for the fluxes of cusp soft electron precipitation based on the upstream solar wind driving conditions.

MITC-04 - Effects of SAPS on thermospheric wind and density during the 17 March 2013 storm - by Cheng Sheng

Status of First Author: Student NOT in poster competition

Authors: Cheng Sheng, Gang Lu, and Wenbin Wang

Abstract: Strong subauroral polarization streams (SAPS) were observed by DMSP satellites during the main phase of the 17 March 2013 geomagnetic storm. TIEGCM simulations have been carried out to investigate the effects of SAPS on thermospheric wind and density. An empirical model of SAPS was incorporated into the TIEGCM, and the SAPS-TIEGCM simulations were compared with the standard TIEGCM run. The influence of SAPS forcing is represented by examining the differences between these two runs. Simulation results were further compared with ion drift and plasma measurements from DMSP as well as with the neutral wind and density measurements from GOCE to assess the model’s performance.

MITC-05 - SAPS simulation with GITM_RCM coupled Model - by Yang Lu

Status of First Author: Student IN poster competition, PhD

Authors: Yang Lu, Yue Deng, Jiapeng Guo, Donghe Zhang, Cheng Sheng, Philip Anderson, and Rodrick Heelis

Abstract: Ion velocity in the Sub Aurora region observed by Satellites in storm time often shows a significant westward component (up to 1000- 2000m/s). The high speed westward stream is distinguished with convection pattern. This kind of events are called Sub Aurora Polarization Stream (SAPS). In March 17th 2013 storm, DMSP F18 satellite observed several SAPS cases when crossing Sub Aurora region. In this study, Global Ionosphere Thermosphere Model (GITM) has been coupled to RCM-UCLA model to simulate the impact of SAPS during March 2013 event on the ionosphere/thermosphere. The particle precipitation and electric field from RCM has been used to drive GITM in the high latitudes. Meanwhile, the newly developed empirical model for SAPS will be coupled to GITM and simulate the effects on upper atmosphere. The comparison of GITM simulations with different SAPS specifications and observations will be conducted as well. To improve the physical understanding, the neutral wind and force terms in the momentum equation will be analyzed.

MITC-06 - Observations of the midlatitude trough and its relationship to subauroral ion drifts (SAID) - by Russell Landry

Status of First Author: Student NOT in poster competition, PhD

Authors: Russell G. Landry, Phillip C. Anderson

Abstract: SAIDs are a phenomena sometimes observed in the subauroral pre midnight ionosphere during magnetically active periods characterized by strong poleward electric fields which drive westward drifts greater than 1 km/s. SAIDs will typically span 1-2 degrees magnetic latitude and several hours in magnetic local time. SAIDs are often observed collocated with the midlatitude trough, and the strong electric field can act to reduce the ionospheric conductivity further through fast chemistry and vertical transport. The theory that SAIDs are generated by ionospheric Pedersen currents fed by field-aligned currents requires the decreased conductance associated with the midlatitude trough to require the latitudinally narrow large amplitude field. Using DMSP satellite measurements from 1987-2012, we are investigating the statistical dependence of the midlatitude trough, as observed at the DMSP 800 km altitude, on season, longitude, and the plasma composition and how these factors effect the likelihood of SAID occurrence.

MITC-07 - Statistical Comparison of the Magnetopause Distance and CPCP for Global MHD Models - by Agnit Mukhopadhyay

Status of First Author: Student IN poster competition, MS

Authors: Agnit Mukhopadhyay

Abstract: Acquiring quantitative metrics-based analysis regarding the performance of most first-principle space physics modeling approaches is key in understanding the solar and space weather. As established by the successive the Geospace Environment Modeling Challenges, quantification of performance help set a precedent in understanding the science behind the various phenomena observed naturally in addition to elucidating the merits and demerits of a space weather prediction method. In this study, the performance of three magnetohydrodynamic models (SWMF/BATS-R-US, LFM and OpenGGCM) in estimating the Earth's magnetopause location and the ionospheric cross polar cap potential (CPCP) have been studied. Using the Community Coordinated Modeling Center's Run-on-Request system and extensive database on

results of various magnetospheric scenarios run during a variety of solar weather patterns, the aforementioned model predictions have been compared with magnetopause standoff distance estimations obtained from six empirical models, and with cross polar cap potential estimations obtained from AMIE and SuperDARN. The events considered in this study contain a spectrum of possibilities – solar storms, substorms, constant solar wind events, which have been categorized using the Kp index as high, moderate and low magnitude solar events. Several of these storms have been well documented as part of the Geospace Environment Modeling (GEM) Challenges and other studies. The root-mean-square difference (RMS), prediction efficiency (PE) and maximum amplitude (Max Amp) metrics are used to quantify the model performances for the solar events considered. A separate metric called Wrong Prediction (WP) has also been used to study the models' hit and miss rates with the empirical data. While almost all the cases considered for the magnetopause standoff distances have a satisfactory performance, there is huge deviation for the CPCP data both in the physics based models and the empirical data. The metric data is therefore valid for the magnetopause location comparisons, while not being that thorough for the CPCP comparative study.

MITC-08 - Low-altitude ion heating with downflowing and upflowing ions - by Yangyang Shen

Status of First Author: Student IN poster competition, PhD

Authors: Yangyang Shen, David Knudsen, Johnathan Burchill, Andrew Howarth, Andrew Yau, Gordon James, David Miles, and Leroy Cogger

Abstract: Mechanisms that energize ions at the initial stage of ion upflow are still not well understood. We statistically investigate ionospheric ion energization and field-aligned motion at very low altitudes (330-730 km) using synergistic plasma, magnetic field, wave electric field and optical data from the e-POP satellite. The high-time-resolution (10 ms) dataset enables us to study the micro-structures of ion heating and field-aligned ion motion. The ion temperature and field-aligned bulk flow velocity are derived from the 2-D ion distribution functions measured by the SEI instrument. From March 2015 to March 2016, we've found 16 orbits (in total 24 ion heating periods) with clear ion heating signatures passing across the dayside cleft or the nightside auroral regions. Most of these events have consistent ion heating and flow velocity characteristics observed from both the SEI and IRM instruments. The perpendicular ion temperature goes up to 4 eV within a ~2 km-wide region in some cases, in which the Radio Receiver Instrument (RRI) sees broadband extremely low frequency (BBELF) waves, demonstrating significant wave-ion heating down to as low as 350 km. The e-POP Fast Auroral Imager (FAI) and Magnetic Field (MGF) instruments show that many events are associated with active aurora and are within downward current regions. Contrary to what would be expected from mirror-force acceleration of heated ions, the majority of these heating events (17 out of 24) are associated with core ion downflow rather than upflow. These statistical results provide us with new sights into ion heating and upflow processes at very low altitudes.

MITC-09 - Swarm Observation of Field-Aligned Currents in Multiple Arc System - by Jiashu Wu

Status of First Author: Student IN poster competition, PhD

Authors: Jiashu Wu, David Knudsen, Eric Donovan, Megan Gillies, and Johnathan Burchill

Abstract: It is often thought that auroral arcs are a direct consequence of upward field-aligned currents. In fact, the relation between currents and brightness is more complicated. Multiple auroral arc systems provide an opportunity to study this relation in detail. In this study, we have identified two types of FAC configurations in multiple parallel arc systems using ground-based optical data from the THEMIS all-sky imagers (ASIs), magnetometers and electric field instruments onboard the Swarm satellites during the period from December 2013 to March 2015. In type 1 events, each arc is an intensification within a broad, unipolar current sheet and downward currents only exist outside the upward current sheet. These type of events are termed "unipolar FAC" events. In type 2 events, multiple arc systems represent a collection of

multiple up/down current pairs, which are termed as “multipolar FAC” events. By collecting 12 events for “unipolar FAC” and 17 events for “multipolar FAC”, we find that (1) “Unipolar FAC” events are mainly located between 22-23MLT. “Multipolar FAC” events are mainly located around midnight. (2) “Multipolar FAC” events are more related to substorm. (3) Arcs in “Unipolar FAC” events have smaller width and separation. (4) Before midnight, the arcs are tilted towards south. After midnight, the arcs are tilted toward north. Future work involves applying ion velocity measure by Swarm Electric Field Instrument (EFI) and establishing a self-consistent relation between FAC, electric fields and ionospheric conductance.

MITC-10 - Impact of the electric field variability on the upper atmosphere during the geomagnetic storm - by Qingyu Zhu

Status of First Author: Student IN poster competition, PhD

Authors: Qingyu Zhu, Yue Deng, Astrid Maute, Art Richmond, Cheng Sheng, and Yanshi Huang

Abstract: Large Poynting flux at the polar cap has been observed by Defense Meteorological Satellite Program (DMSP) satellites during the August 5-6, 2011 storm event, which is comparable to the Poynting flux in the aurora zone. One candidate mechanism for the enhanced Poynting flux at the polar cap is the small-scale electric field variability. In order to evaluate the contribution from the small-scale electric field variability to the Poynting flux enhancement at the polar cap during this event, a recently developed empirical model for high-latitude electric field variability has been coupled into global ionosphere and thermosphere model (GITM). Altitudinal-integrated Joule heating from GITM with/without the electric field variability along the DMSP trajectory has been compared with DMSP Poynting flux observation. Furthermore, the impact of the heating associated with the small-scale electric field variability on the thermosphere during this event has been examined by evaluating the neutral mass density from GITM simulation after adding the small-scale electric variability.

PLANETARY STUDIES

PLAN-01 - Comparative Aeronomy: Molecular Ionospheres at Earth and Mars - by Michael Mendillo

Status of First Author: Non-student, MA

Authors: Michael Mendillo, Jeffrey Trovato, Clara Narvaez, Majd Mayyasi, Luke Moore, Marissa F. Vogt, Kathryn Fallows, Paul Withers, and Carlos Martinis

Abstract: The ionospheres in our solar system vary not only in their electron densities, but also in the dominance of atomic versus molecular ions at their altitudes of peak plasma density. With the exception of Earth's F-layer composed of atomic oxygen ions and electrons, all other planets have their peak ionospheric layers composed of molecular ions and electrons embedded in a dense neutral atmosphere. At Mars, both of its ionospheric layers have molecular ions, with the M1-layer at a lower altitude than the more robust M2-layer above it. The terrestrial ionosphere has a prominent region of molecular ions (the E-layer) below the dominant F-layer. In this paper, we explore the production and loss of molecular ion layers observed under the same solar irradiance conditions at Mars and Earth. We compare observations of M1 and M2 electron densities with terrestrial ionosonde data for the peak densities of the E- and F-layers during low, moderate and high solar flux conditions. The sub-solar peak densities of molecular ion layers have high correlations at each planet, as well as between planets, even though they are produced by separate portions of the solar spectrum. We use photo-chemical-equilibrium theory for layers produced by soft X-rays (M1 and E) versus the M2-layer produced by extreme ultraviolet (EUV) to identify the key parameters that cause similarities and differences. The yield of our comparative study points to the roles of

secondary ionization and temperature dependent plasma recombination rates as areas most in need of further study at each planet.

PLAN-02 - Using the Development Process of the Venus Global Ionosphere-Thermosphere Model to Understand the Importance of Planetary Attributes on Earth's Atmosphere - by Emily Judd

Status of First Author: Student IN poster competition, PhD

Authors: Emily L. Judd, Aaron Ridley

Abstract: The Global Ionosphere-Thermosphere Model (GITM) has been used to model the atmosphere of Earth, with various versions for studies of Mars, Jupiter, and Titan. Currently, a version for Venus is under development. During this process, we are conducting systematic studies of how the Earth's atmosphere changes when given certain characteristics of Venus. The Venus model (V-GITM) development includes systematic parameter variances of certain key planetary attributes such as distance from the Sun, planetary axis tilt, and rotation and solar-orbital rates. The lack of an intrinsic magnetic field will also be implemented, along with an atmospheric composition of high carbon dioxide levels and different ratios of minor species. This methodical approach to creating an atmospheric model of Venus will allow for a closer look at the importance of planetary characteristics on Earth's atmosphere. The results from these studies will be presented in the poster.

POLAR AERONOMY

POLA-01 - Kinetic modeling of auroral ion Outflows observed by the VISIONS sounding rocket - by Robert Albarran

Status of First Author: Student IN poster competition, PhD

Authors: R. Albarran, M. Zettergren, D. Rowland, J. Klenzing, and J. Clemmons

Abstract: The VISIONS (VISualizing Ion Outflow via Neutral atom imaging during a Substorm) sounding rocket was launched on Feb. 7, 2013 at 8:21 UTC from Poker Flat, Alaska, into an auroral substorm with the objective of identifying the drivers and dynamics of the ion outflow below 1000km. Energetic ion data from the VISIONS polar cap boundary crossing show evidence of an ion "pressure cooker" effect whereby ions energized via transverse heating in the topside ionosphere travel upward and are impeded by a parallel potential structure at higher altitudes. VISIONS was also instrumented with an energetic neutral atom (ENA) detector which measured neutral particles (~50-100 eV energy) presumably produced by charge-exchange with the energized outflowing ions. Hence, inferences about ion outflow may be made via remotely-sensing measurements of ENAs. This investigation focuses on modeling energetic outflowing ion distributions observed by VISIONS using a kinetic model. This kinetic model traces large numbers of individual particles, using a guiding-center approximation, in order to allow calculation of ion distribution functions and moments. For the present study we include mirror and parallel electric field forces, and a source of ion cyclotron resonance (ICR) wave heating, thought to be central to the transverse energization of ions. The model is initiated with a steady-state ion density altitude profile and Maxwellian velocity distribution characterizing the initial phase-space conditions for multiple particle trajectories. This project serves to advance our understanding of the drivers and particle dynamics in the auroral ionosphere and to improve data analysis methods for future sounding rocket and satellite missions.

POLA-02 - Imaging Fabry-Perot Observations of Thermospheric Dynamics in Antarctica - by Mark Conde

Status of First Author: Non-student

Authors: John Elliott, Riley Troyer

Abstract: During the austral summer of 2015-2016 the Geophysical Institute of the University of Alaska Fairbanks installed all-sky imaging Fabry-Perot spectrometers in Antarctica at the United States' South Pole and McMurdo Sound research stations. Both of these sites are located at geomagnetic latitudes corresponding to the equatorward edge of the polar cap under quiet to moderate levels of geomagnetic activity. As of June 2017, they have each collected 1.5 seasons of observational data. Between 2007 and 2014 the South Pole instrument was located at a different site: Mawson, Antarctica. Mawson is at a lower geomagnetic latitude and lies within the auroral oval during quiet to moderate levels of activity. These data sets allow us to compare how the transition from the auroral oval to the polar cap affects thermospheric wind circulation under a range of activity levels. The behavior of this transition will be illustrated by comparing the historical Mawson wind observations with data now being collected from McMurdo and South Pole.

POLA-03 - Statistical Characteristics of Ionospheric Polar Cap Patches Observed by RISR-C - by Jiaen Ren

Status of First Author: Student IN poster competition, PhD

Authors: Jiaen Ren, Shasha Zou

Abstract: Polar cap “patches” are 100-1000 km islands of high-density plasma (at least double the density of surrounding background) which can cause scintillation and outages of space communications and degraded performance for Global Navigation Satellite System (GNSS) at polar latitudes. Mitigation techniques are limited because we are still not clear about what governs the generation, propagation and ultimate fate of most observed patches. Measurements of ionospheric plasma properties with adequate temporal resolution and spatial coverage will provide key information in the study of the highly-debated patches production mechanisms and transpolar evolution process.

The proposed research investigates the statistical characteristics of the polar cap patches, including their occurrence rates distribution over magnetic local time and their average vertical profiles of multiple plasma properties. The study uses the measurements of electron density and temperature, ion temperature and velocity from the Resolute Bay Incoherent Scattered Radar – Canada (RISR-C) and complementary instruments, including simultaneous measurements of solar wind by ACE and WIND spacecraft. Results show high electron density, low electron temperature and upward ion flow within the observed polar cap patches, which have a peak of occurrence rate near the afternoon sector. The statistical features of the polar cap patches can provide new insights on our understanding about how the plasma patches are produced and transported across the polar cap.

POLA-04 - Seasonal dependence of geomagnetic active time northern high-latitude upper thermospheric winds - by Manbharat Dhady

Status of First Author: Non-student

Authors: John Emmert, Douglas Drob

Abstract: We present initial results of a study of the synoptic scale seasonal dependence of northern high-latitude F-region thermospheric winds under active geomagnetic conditions. The analysis combines extensive observations of thermospheric winds recorded by eight ground-based (optical remote sensing) and three space-based (optical remote sensing and in-situ) instruments at northern high latitudes. These data

sets provide enough high-latitude geospace coverage to develop a seasonal empirical representation of vector winds as a function of season, magnetic latitude, and magnetic local time. This empirical morphology accurately represents the behavior of its constituent datasets. The assimilated wind patterns exhibit a strong and large duskside anticyclonic circulation cell, a weak dawnside cyclonic circulation cell, sharp latitudinal gradients on the duskside, and strong antisunward winds in the polar cap. The duskside circulation is strongest in summer and weakest in winter; its latitudinal extent expands from winter to summer. The dawnside circulation appears to weaken from winter to equinox to summer. The westward zonal winds channeling through the auroral zone on the duskside and meridional winds in the polar cap show strong intensification from winter to summer. Relative to corresponding quiet-time patterns, the perturbation winds also exhibit strong seasonal variability which decreases with decreasing latitude. Similarities in the perturbed winds of Disturbed Wind Model (DWM07) and summer perturbed winds derived here suggest that DWM07 winds are skewed toward summer conditions.

POLA-05 - Characterizing the Polar Topside Ionosphere - by Aaron Bunch

Status of First Author: Student IN poster competition, BS

Authors: Aaron Bunch, Roger Varney

Abstract: We undertake a full-profile analysis of incoherent scatter radar data from RISR-N and RISR-C in order to characterize the polar topside ionosphere between 160 km and 1664 km. Preliminary results show reliable values for electron density up to 800 km, but they also pose several challenges: (1) Above 800 km the electron density parameter is affected by satellites that are difficult to clean from the data. (2) The most expensive part of the forward model calculation is computed on a lower-resolution intermediate grid. All the model parameters (especially above 800 km) are sensitive to the resolution of this grid. (3) Without heavy-handed fitting penalties, the electron temperature falls to zero above 800 km, and the ion temperature varies wildly depending on the resolution of the intermediate grid.

POLA-06 - Occurrence of ion upflow associated with ion/electron heating in the polar cap and cusp regions - by Eun-Young Ji

Status of First Author: Non-student,

Authors: Geonhwa Jee, Young-Sil Kwak, Changsup Lee, and Jeong-Han Kim

Abstract: In this study, we investigate the occurrence frequency of ion upflow associated with ion/electron heating in the polar cap and cusp regions, using the data obtained from the European Incoherent Scatter Svalbard radar (ESR) between 2000 and 2010. We classify the upflow events by four cases: driven by ion heating (case 1), electron heating (case 2), both ion and electron heatings (case 3), and without any heating (case 4). The statistical analysis of the data shows that the upflow normally starts at around 350 km altitude and the occurrence seems to peak at 11 MLT. Among the four cases, the occurrence frequency of the upflow is maximized for the case 2 and then followed by case 4, case 1 and case 3. At around 500 km altitude, however, the occurrence frequency is maximized when there is no heating (case 4). We also investigate the dependence of the occurrence frequency of the upflow on Kp and F10.7 indices. The moderate geomagnetic condition ($2 \leq Kp < 5$) seems to show maximum occurrence frequency. As for the solar activity, the occurrence frequency is higher for low solar activity than for high solar activity. The results of this study suggest that the ion upflow occurring in the polar cap/cusp region is mostly driven by electron heating associated with soft particle precipitation.

POLA-07 - Exploring the high-latitude thermosphere responses to IMF By reversal - by Dongjie Guo

Status of First Author: Student IN poster competition, PhD

Authors: Dongjie Guo, Aaron Ridley, and Jiuhou Lei

Abstract: The Global Ionosphere-Thermosphere Model (GITM) is used to investigate the thermosphere responses to a sudden interplanetary magnetic field (IMF) By reversal. Two ideal simulations with and without IMF By reversal from about 5 nT to -5 nT are conducted during the March equinox. The average temperature of the northern high-latitude thermosphere at 400 km increases rapidly from about 1500 K to 1550 K in roughly half an hour after the By reversal, which results in a corresponding increase of the average density from about 6.6×10^{-12} kg/m³ to 6.8×10^{-12} kg/m³. Then both the average temperature and density decrease with time, and they become even smaller than the simulation results without By change 2.5 hours after the By reversal. Our simulation results at 400 km also give a low thermospheric density around the dawnside sector in the northern hemisphere. This density low structure is always located at the center of the neutral vortex. After the By reversal, this structure gets weakened at first, and it nearly disappeared about 1.5 hours later. However, this structure emerges again after the disappearance and gets even stronger later on. Our results suggest that the response of the thermospheric density to IMF By reversal can be affected by both the thermospheric temperature and wind pattern through Joule heating and ion-neutral momentum transfer processes at the high latitudes. And the neutral wind convection pattern may need a longer time to respond to the By change than the temperature does.

POLA-08 - Measuring F-region ion-neutral coupling in response to increases in auroral precipitation - by Andrew Kiene

Status of First Author: Non-student

Authors: A. Kiene, W. A. Bristow, M. Conde, and D.L. Hampton

Abstract: Neutral winds are a key factor in the dynamics of the ionosphere-thermosphere system. Previous observations have shown neutral and ion flows to be strongly coupled during periods of auroral activity, but this coupling is suppressed when aurora is not present. This is primarily due to enhanced particle precipitation during auroral activity. Current simulations have difficulty reproducing momentum coupling on large scales due to the sensitivity of modeled winds to particle precipitation inputs. It is therefore critical to both accurately measure auroral precipitation as well as the resulting increase in the ion-neutral coupling. Recent advancements in high-resolution fitting of SuperDARN data have enabled us to generate a steady map of ion drifts over Alaska, coinciding with several optics sites. Available optical instruments include digital all-sky imagers and meridian spectrographs, which provide measurements of auroral intensity at three wavelengths. Also present are several Scanning Doppler Imagers, which can measure thermospheric winds and temperatures over a wide area. In this study, we have combined these three data sets in order to investigate the impact of increases in particle precipitation on ion-neutral coupling. We have found a significant correlation between enhancements auroral emission resulting from precipitation and increases in the ion-neutral coupling in the pre-magnetic midnight sector. In addition, we have quantified the time scale over which the coupling occurs, comparing our observations to previous theoretical estimates.

POLA-09 - Thermospheric wind variations at substorm onset: Multi-event study using a Fabry-Perot interferometer at Tromsø, Norway - by Heqiucen Xu

Status of First Author: Student IN poster competition, MS

Authors: Heqiucen Xu, Kazuo Shiokawa, Shin-ichiro Oyama and Yuichi Otsuka

Abstract: In this study, we focused on the thermospheric wind variations at the onset of isolated substorms. Substorms input energy into the ionosphere from the magnetosphere, during which the high-latitude ionosphere and thermosphere are severely influenced. The ionospheric responses to substorms such as during the recovery phase have been investigated by Oyama et al. [2016]. One purpose of this study is to find the characteristics of thermospheric wind variations at the substorm onset. At the same time, we expect to investigate the possibility that wind variations as a potential driver of substorm-onset-related ionospheric current system according to the magnetosphere-ionosphere coupling substorm model [Kan, 1993]. A Fabry-Perot interferometer (FPI) at Tromsø of Norway provided us with wind

observations from Doppler shift of both red-line (630.0 nm for the F region) and green-line (557.7 nm for the E region) emissions of aurora and airglow. We used seven-year data from 2009 to 2015 with a time resolution of ~ 13 min. We first identified the onset times of local isolated substorms by using ground-based magnetometer data of the IMAGE magnetometer chain obtained at the Tromsø and Bear Island stations. Totally, we obtained 4 red-line events and 5 green-line events located at different local times. For all these events, the peaks of westward ionospheric currents are located at the north of Tromsø. Then, we calculated two weighted averages of wind velocities at ± 15 min of the onset time and 30-min after the onset time of substorms. We used the difference between these two weighted averages to indicate the strength of wind changes. As a result, the observed wind changes at these substorm onsets were less than 49 m/s for red-line events, and 26 m/s for green-line events. These wind changes are much smaller than the typical plasma convection speed, indicating that the plasma motion caused by thermospheric wind through ion-neutral collision is a minor effect as the driver of high-latitude plasma convection, as well as the triggering of substorm onset according to the magnetosphere-ionosphere coupling substorm model. We discuss the possible causes of the observed wind changes at the onset of substorms by using line-of-sight winds of the FPI sky scan, both north-south and east-west keograms of all-sky auroral images at Tromsø, and IMF-associated plasma convection pattern.

POLA-10 - High Resolution Case Studies of Giant Auroral Undulations - by Michael Ahrns

Status of First Author: Student NOT in poster competition, PhD

Authors: Jason Ahrns, Donald Hampton, and William Bristow

Abstract: Giant Auroral Undulations, a north/south quasiperiodic wave structure in the equatorial edge of the auroral zone, have been reported in the literature for a few years, but most observational information is limited to satellite overpasses (poor time resolution) or few events. We report several events, recorded with high temporal and spatial resolution and supported by simultaneous radar and spectrometer data, that add some understanding of the typical characteristics of GAUs. Previous papers have discussed GAUs as a proton aurora phenomenon, and this has informed discussions of its potential mechanisms. Our dataset, including spectrometer observations of GAUs and high time resolution allsky camera observations of pulsating bands within the GAUs, suggest GAUs can also appear in the equatorward electron boundary. This is important when considering possible GAU mechanisms.

POLA-11 - Preliminary Data Analysis of ISINGLASS Campaign Launches - by Robert Clayton

Status of First Author: Student NOT in poster competition, PhD

Authors: Robert Clayton, Kristina Lynch

Abstract: We are presenting a first look at the data from the ISINGLASS campaign rockets from February and March of 2017. In situ measurements of electron temperature, ion flow, and electric field are combined with a background picture from ground based cameras, radar data, and magnetometer data to describe the behavior of an auroral arc in a localized region. The ground based measurements provide context in the form of a greater localized picture of the event region, while the high cadence in situ data provides insight into the small scale physics inside the auroral arcs and the arc boundaries. Processed data from all sources will be assimilated with a model for interpretation of the events. Specifically in situ DC electric field information and auroral arc boundaries from camera data are of interest for interpretation.

SOLAR TERRESTRIAL INTERACTIONS IN THE UPPER ATMOSPHERE

SOLA-01 - Tomographic estimation of exospheric hydrogen density distributions - by Gonzalo Cucho-Padin

Status of First Author: Student IN poster competition, PhD

Authors: Gonzalo Cucho-Padin, Lara Waldrop

Abstract: For the past decade, the Lyman-alpha detectors (LADs) onboard NASA's Two Wide-angle Imaging Neutral-atom Spectrometers (TWINS) mission have obtained routine measurements of solar Lyman-alpha photons (121.6nm) resonantly scattered by atomic hydrogen (H) in the terrestrial exosphere. This data has been used to derive global, 3-D models of exospheric H density beyond 3 Re, which are needed to understand the influence of solar activity and ion-neutral coupling throughout the terrestrial environment as well as to assess its long-term evolution through atmospheric escape. These historical models are based on parametric fitting of assumed functional forms which may be inaccurate or invalid, thus limiting confidence in conclusions drawn from analysis of the resulting distributions. In this work, we present a new means of global, 3D reconstruction of exospheric H density through a tomographic inversion of the scattered H Lyman-alpha emission. Our approach avoids the conventional dependence on ad hoc and arbitrary parametric formulations and enables a more accurate characterization of the global structure of this region. We evaluate the feasibility of the new technique using both simulated and actual TWINS data and report new geophysical insights gained from this promising approach.

SOLA-02 - Studying the response of the low-ionosphere to solar Long Duration Gamma-Ray Flares (LDGRF) - by Alessandra Abe Pacini

Status of First Author: Non-student

Authors: A.A.Pacini (APL/JHU)

Abstract: In this work, we investigate the impact of a special type of Solar Flare on the low ionosphere registered in the VLF data. The studied solar flares present an extended high-energy gamma-ray emissions (> 50 MeV) after their impulsive phase, while other common flare emissions (including hard X-rays) are already absent or significantly diminished. The gamma emission from this kind of flares, known as LDGRF – Long Duration Gamma-Ray Flares, is believed to originate from the decay of pions, produced by protons > 300 MeV and alpha-particles > 200 MeV interacting deep in the solar atmosphere of the active region (but the solar origins of this high-energy extended gamma-ray events are not completely understood yet). Fermi/LAT recently identified more than twenty such flares with γ -ray emission > 100 MeV, many of which exhibit emission from 30 minutes to tens of hours in duration (before 2008, only 13 LDGRF events had been identified). Because of the Fermi sensitivity, the once rare high-energy emission flare is apparently more common than previously thought. In order to improve the statistics of LDGRF studies, it would be essential to have a proxy with long time coverage. Once we can characterize the LDGRF imprints in the VLF signal, we'll be able to identify solar events not observed by Fermi/LAT using the ionosphere as a big detector of high-energy solar events and associate them with other solar data (like RHESSI) constraining the existent acceleration models. The analysis presented here represents the first effort that will allow the use of the low ionosphere as a detector (proxy) for the LDGRF high-energy emissions.

SOLA-03 - Effects of Space Weather on the Estimation of Thermospheric Density - by Timothy Kodikara

Status of First Author: Student IN poster competition, PhD

Authors: Timothy Kodikara, Brett Carter, Robert Norman, and Kefei Zhang

Abstract: A prime requirement for the management of satellites, space-based services and technologies is to be able to precisely track and predict the orbit of satellites and any other objects in the environment. More than half of the total Earth-orbiting satellite population is in the 160–2000 km altitude range (LEO) with a commercial value in the order of hundreds of billion USD. The largest uncertainty in orbit tracking and prediction in the LEO region originates from the poor estimation of atmospheric drag. While many parameters contribute to atmospheric drag, in near-Earth space (160–800 km) the largest source of error is in the modelling of air density (atmospheric mass density, AMD). The modelling error of AMD is regarded to be around 15–20%. This error needs to be brought down to below 5% to reliably predict the orbit, 1–2 days in advance.

A preliminary validation of thermospheric neutral densities derived from Swarm satellite observations is also presented. In general, a considerable incongruity exists between Swarm observations for 2014 and simulations. The findings highlight the need to address disturbances in Swarm accelerometer data and as well as better representation of lower-atmospheric processes that engender perturbations in the thermosphere, and space weather activity in the model. An analysis of certain such processes has been provided with a quantification of the influence of lower-atmospheric forcing on different empirical convection models. A complete theoretical explication of the causation of seasonal variations, however, remain a challenge.

SOLA-04 - Initial Validation of CTIPe Neutral Winds using GOCE Satellite Observations - by Mariangel Fedrizzi

Status of First Author: Non-student

Authors: M. Fedrizzi, E. Doornbos, T.J. Fuller-Rowell, M. Codrescu, and V. Yudin

Abstract: Thermospheric winds are one of the main sources of variability in the thermosphere-ionosphere (T-I) system. Neutral winds in the thermosphere have been studied extensively using ground-based, in situ and remote sensing satellite data, leading to a reasonably good understanding of their climatology and to a development of empirical and numerical general circulation models. The validation of the dynamics of the best available physics-based models has been far from comprehensive. The challenge for the future is to quantitatively characterize the thermospheric dynamics and the global circulation, which requires detailed analysis of observations on the dynamics itself and its impact on the T-I system, guided by numerical models. This work presents initial comparisons of thermospheric neutral winds obtained from a self-consistent physics-based coupled model of the thermosphere, ionosphere, plasmasphere and electrodynamics (CTIPe) with GOCE (Gravity field and steady-state Ocean Circulation Explorer) satellite high precision accelerometers measurements to assess quantitatively the capabilities and limitations of the model, and advance the understanding of the T-I system dynamics on different spatial and temporal scales.

SOLA-05 - Ionosphere-thermosphere modeling in a forecastable mode: case study of the June 2012 geomagnetic storm - by Xing Meng

Status of First Author: Non-student

Authors: X. Meng, A. J. Mannucci, O. P. Verkhoglyadova, B. T. Tsurutani, and R. M. McGranaghan

Abstract: This study addresses the current capability of forecasting the ionosphere-thermosphere system using first-principles models. As an interesting example, we examine the June 2012 geomagnetic storm, induced by a high-speed solar wind stream. We perform numerical simulations with the Global Ionosphere-Thermosphere Model (GITM) in a forecastable mode, i.e., the drivers can be predicted a few days ahead. By comparing the modeling results to available in-situ and remote-sensing observations of the total electron content, neutral wind, composition, etc., we evaluate the modeling performance and investigate causes of model-data disagreement. We will provide insight on factors affecting accurate forecasts of ionospheric-thermospheric responses to geomagnetic disturbances.

SOLA-06 - Statistical study of the traveling ionospheric disturbances generated by solar terminator based on Dynasonde data - by Huan Song

Status of First Author: Student NOT in poster competition, PhD

Authors: Huan Song; Nikolay Zabolin; and Terence Bullett

Abstract: Solar terminator represents a unique source of atmospheric waves possessing of near-ideal coherent properties: its geometry and magnitude of the impact changes very little from day to day. This feature has been used in [Forbes et al., GRL, 2008] to obtain "snapshots" of terminator waves in the neutral atmosphere at the altitude 400 km by averaging CHAMP accelerometer data over long sequences of the satellite passes. The results were represented in the geographic latitude vs local time coordinates. We apply a similar approach averaging time series of Wallops Island, VA Dynasonde Doppler data to obtain "snapshots" of terminator waves in the ionosphere in the true altitude vs local time coordinates. The averaging is performed independently for every month of the year-long observation period from May 2013 to April 2014. The altitude range covered is 90 km to 400 km with 1 km resolution, representing the entire bottom-side ionosphere. Individual local time segments used for the averaging were 12 hours long and all centered on the times of the dawn or dusk terminator passing at every specific altitude. This approach effectively suppresses all kinds of incoherent wave activity and allows one to reveal the perturbation phenomenon mainly caused by the solar terminator. Both dawn and dusk terminator waves can be easily observed in majority of the monthly images. The phase fronts of the dusk terminator wave are propagating downward indicating upward movement of the terminator-related disturbance and of the wave generated by it. The phase fronts of the dawn terminator waves are propagating upward indicating downward movement of the terminator-related disturbance and of the wave generated by it. Spectral analysis of the local time sequences reveals characteristic peaks in the terminator wave activity corresponding to the periods 30-36 min, 1 hour and 2 hours and a continuum component.

SOLA-07 - Analysis of the August 2017 Eclipse's Effect on Radio Wave Propagation Employing a Raytrace Algorithm - by Magdalena Moses

Status of First Author: Student NOT in poster competition, MS

Authors: Magdalena Moses, Sushma Burujupalli, Snehal Dixit, Lee Kordella, Charudatta Chitale, and Gregory Earle

Abstract: The upcoming total solar eclipse over the continental United States on August 21 offers a unique opportunity to study the dependence of the ionospheric density and morphology on incident solar radiation. There are significant differences between the conditions during a solar eclipse and the conditions normally experienced at sunset and sunrise, including the west-to-east motion of the eclipse terminator, the speed of the transition, and the continued visibility of the corona throughout the eclipse interval. Taken together, these factors imply that unique ionospheric responses may be witnessed during eclipses, reflected by changes in radio frequency (RF) propagation at high frequency (HF). In order to predict these changes, we employ the HF propagation toolbox, PHaRLAP, created by Dr. Manuel Cervera. We use an eclipsed ionosphere model to study propagation along the eclipse path over the course of the eclipse. Analysis of eclipse RF propagation and ionosonde data guided by the results of these raytracing algorithms will help us understand the underlying processes governing the ionosphere, and improve our model of the F-Region responses to an eclipse.

Abe Pacini,Alessandra, 30
Ahrns,Michael, 29
Albarran,Robert, 25

Bhaneja,Preeti, 12
Branning,Kylee, 16
Brown,Steven, 17
Bunch,Aaron, 27
Burleigh,Meghan, 20

Chakraborty,Shibaji, 8
Chiu,Pei-yun, 9
Clayton,Robert, 29
Conde,Mark, 26
Cucho-Padin,Gonzalo, 30

Dang,Tong, 21
Derghazarian,Sevag, 3
Desai,Abhishek, 7
Dhadly,Manbharat, 26

Evonosky,William, 6

Fallen,Christopher, 9
Fang,Tzu-Wei, 3
Fedrizzi,Mariangel, 31
Finan,Robert, 14
Flynn,Sierra, 1
Franco-Diaz,Eframir, 15

Guo,Dongjie, 27

Han,Xiaoyu, 12
Hickey,Dustin, 9
Hsu,Chih-Ting, 2

Inonan,Marcos, 13

Ji, Eun-Young, 27
Johnsrud,Torfinn, 19
Joshi,Dev.,10
Joshi,Pratik, 17
Judd,Emily, 25

Khadka,Sovit, 6
Kiene,Andrew, 28
Kilcommons,Liam, 1
Kodikara,Timothy, 30

Landry,Russell, 22
Lee,Wookyoung, 4
Lien,Chuan-Ping, 4
Lu,Yang, 22

Maimaiti,Maimaitirebike, 18
Mathew,Tiju, 7
Maute,Astrid, 5
Mendillo, Michael, 24
Meng,Xing, 31
Moses,Magdalena , 32
Mrak,Sebastijan, 11
Mukhopadhyay,Agnit, 22

Navarro, Luis, 4
Nossa,Eliana, 16
Nossal,Susan, 14

Phal,Yamuna, 15

Qin,Jianqi, 20

Reimer,Ashton, 2
Ren,Jiaen, 26

Santos,Pedrina, 17
Seif,Aramesh, 10
Shen,Yangyang, 23
Sheng,Cheng, 21
Shi,Yining, 2
Shidler,Sam, 5
Smith,Jonathon, 12
Song,Huan, 32
Su,Yang, 13

Tsai Lin,Rong, 16

Valdez Portocarrero,Alexander, 8

Wang,Ningchao, 19
Wu, Jiashu, 23

Xu,Heqiucen, 28

Zhan,Weijia, 14
Zhang,Kedeng, 18
Zhu,Qingyu, 24